國 立 交 通 大 學

電子工程學系 電子研究所碩士班

碩 士 論 文

用於 UWB 及 WIMAX 之雙模
通道等化器設計

Dual mode Channel Equalizer Design
for UWB and WIMAX Systems

研 究 生：葉柏麟　　Po-Lin Yeh

指導教授：溫瓌岸　博士　　Dr. Kuei-Ann Wen

中 華 民 國 九 十 七 年 七 月

用於 UWB 及 WIMAX 之雙模
通道等化器設計

Dual mode Channel Equalizer Design
for UWB and WIMAX Systems

研 究 生：葉柏麟　　Student： Po-Lin Yeh

指導教授：溫瓌岸 博士　　Advisor： Dr. Kuei-Ann Wen

國 立 交 通 大 學

電子工程學系 電子研究所碩士班

碩 士 論 文

A Thesis
Submitted to Department of Electronics Engineering & Institute of Electronics
Electronics College of Electrical and Computer Engineering
National Chiao Tung University
in Partial Fulfillment of the Requirements
for the Degree of Master
in
Electronic Engineering
July 2008

中 華 民 國 九 十 七 年 七 月

於 UWB 及 WIMAX 之雙模
通道等化器設計

研究生：葉柏麟　　指導教授： 溫瓌岸博士

國立交通大學

電子工程學系　　電子研究所碩士班

摘要

本論文提出一適用於 IEEE 802.15.3a 與 IEEE 802.16d 雙規格的通道等化器，此通道等化器包含通道估測，頻域等化器，相位追蹤器，適應性通道追蹤器等，用以解決正交分頻多工系統上，存在之多路徑通道，加成性白色高斯，射頻傳輸器與接收器之本地訊號不匹配以及 D/A 與 A/D 之取樣頻率不匹配等非理想效應。

經由完整的 UWB 系統模擬，所提出的方法在不同的傳輸環境下，可達到 1.36~7.25dB 的 SNR 系統效能增益，WIMAX 的系統方面，另提出的適應性通道追蹤器，可有效減少通道估測誤差，經由模擬，提出的方法可降低 3~18 dB 的通道估測方均誤差(MSE)，在不同的傳輸環境下，也可獲得 0.5~3.9dB 的 SNR 系統效能增益。

為了處理雙模的訊號，採用了通用於兩種系統規格的演算法，電路設計上得以運用通用的運算單元，以提升使硬體使用效率，藉由 Synopsys Design Complier 合成，在 UMC 0.18 um CMOS 的製程環境下，所提出的設計僅需 13 萬邏輯閘，另外為了符合 UWB 528Msamples/s 的資料處理速度，電路上採用了兩倍平行度的設計，使其輸出量最快可達到 540 百萬取樣。

Dual mode Channel Equalizer Design for UWB and WIMAX Systems

Student: Po-Lin Yeh Advisor: Dr. Kuei-Ann Wen

Department of Electronics Engineering Institute of Electronics

National Chiao-Tung University

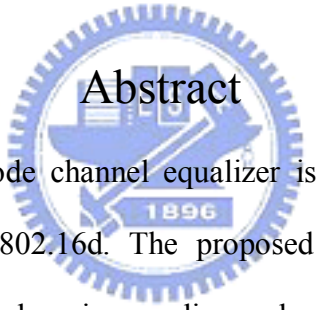

Abstract

In this thesis, a dual mode channel equalizer is proposed for applications on IEEE 802.15.3.a and IEEE 802.16d. The proposed channel equalizer comprises channel estimator, frequency domain equalizer, phase error tracker, and adaptive channel tracker. It is applied to resolve non-ideal effects, such as multi-paths channel, additive white Gaussian noise, carrier frequency mismatch between RF transmitter and receiver, sampling clock mismatch between digital-to-analog converter and analog-to-digital converter in Orthogonal Frequency Division Multiplexing (OFDM) system.

Through complete UWB simulation, the proposed channel equalizer can obtain 1.36 ~7.25dB gain in signal-to-noise ratio (SNR) for different transmission conditions. In WIMAX system, the proposed adaptive channel tracker can reduce channel estimation error effectively. With system simulation, the proposed adaptive channel tracker can reduce the mean-square-error of channel estimation by 3~18 dB. Under

different transmission conditions, the proposed methodology can obtain 0.5~3.9 dB SNR gain.

In order to deal with dual-mode signals, common algorithms are selected to process both UWB and WIMAX signals. With common Algorithms, common architectures can be designed to obtain hardware efficiency. Design is synthesized to UMC 0.18um CMOS standard cell technology library with Synopsys Design Compiler. The total gate count is merely 130k. Finally, in order to meet the sampling rate of 528Msample/s for UWB, the proposed channel equalizer uses two-parallelism and throughput can achieves 540M samples per second.

誌 謝

首先，第一個要感謝的是指導教授，溫瓌岸教授。感謝老師在兩年研究生涯中，不斷的給予柏麟指導與督促。溫老師的教誨，讓學生在學習訓練的路途上，能夠快速而正確的修正自己的研究方向，並且保持不鬆懈的心態進行研究，也感謝TWT_LAB 在這兩年中提供的豐富研究資源，讓我在研究上無後顧之憂，感謝實驗室的學長們的指導與照顧:彭嘉笙，溫文燊，林立協，陳哲生，鄒文安，廖俊閔，張懷仁，蔡彥凱，莊翔琮，林義凱，吳家岱，梁書旗，李漢建，侯閎仁。感謝兩年來一起打拚的同學:黃俊彥，黃謙若，楊士賢，林佳欣，黃國爵，王磊中。大家在生活上的互相扶持與鼓勵，讓原本辛苦煩悶的研究工作，也變的輕鬆愉快許多。

同時也要感謝實驗室的助理:翁淑怡，陳宛君，張嘉誠，魏智伶，陳恩齊，陳慶宏，有妳們幫忙處理實驗室的雜務，才能讓我們能夠專心致力於研究。感謝默默支持我的家人，爸爸，媽媽，哥哥。你們不斷的支持與鼓勵，讓我覺得需要更努力來回報你們。最後，感謝可愛與聰明的女朋友先俐，陪我度過兩年的歲月.

葉柏麟 2008 年 7 月

Contents

List of Tables

List of Figures

Chapter 1.
Introduction

In this chapter, the motivation of this research and basic concepts of OFDM are introduced. Then, the system specification of OFDM-based UWB and WIMAX systems will be introduced.

1.1. Motivation

Orthogonal frequency division multiplexing (OFDM) is a multi-carrier transmission. It is a very popular technology in recent years. It can deal with multi-path channel effectively in wireless communication systems. Also, OFDM system can provide higher data rate transmission, and higher efficiency of bandwidth utilization.

UWB which adopts OFDM technology is built for future digital home application. Because it offers high-rates in short distance, so consumer can share multimedia in WPAN, including large screen displays, speakers, televisions, digital video recorders, digital cameras, smart phones and more. The constitution of UWB standard provides transmission of high quality multimedia signal. WIMAX which adopts OFDM technology is the best solution for Broadband Wireless Metropolitan Area Networks. Except to the metropolitan area, WIMAX can also provide suburban area with high speed wireless transmission. WIMAX technology resolves the problem of “last mile”. The constitution of this standard, eliminate the huge cost to build up fiber, and boost the efficiency of economy.

A dual-mode device which supports these two applications can combine

common feature of two systems, reducing the wastage of resource, and afford the better service. Channel equalizer is the most important part in OFDM system. Consequently, the object of this thesis is to design a dual-mode channel equalizer which can be applied to UWB and WIMAX systems

1.2. Introduction to OFDM system

The basic principle of OFDM is to split the available spectrum into many orthogonal sub-carriers and transmit them simultaneously [1]. OFDM is very similar to traditional Frequency Division Multiple Access (FDMA). But, by way of the applied orthogonal technology, the usage of spectrum is more efficiency. Otherwise, OFDM system is robust to against multi-path fading channel, because the extension of symbol duration and the guard time introduced between OFDM symbols. OFDM system uses Fast Fourier Transform (FFT) and Inverse Fourier Transform (IFFT) to make the sub-carriers orthogonal with each other. With this technology, the influence of inter-carrier interference (ICI) can also be eliminated. Due to these advantages of low multi-path distortion and high spectral efficiency, OFDM is widely used in several communication systems, such as DAB, DVB, WLAN, UWB, WIMAX.

OFDM system use parallel-transmitted orthogonal sub-carriers. As an example, Fig. 1.1 shows three sub-carriers from one OFDM signal. In this example, all sub-carriers have the same phase and amplitude, but in practice the amplitudes and phases may be modulated differently for each sub-carrier. As it can be shown in Fig. 1.1, each sub-carrier has exactly an integer number of cycles in the interval T, and the number of cycles between adjacent sub-carrier differs by exactly one. This is the property of orthogonality between the sub-carriers.

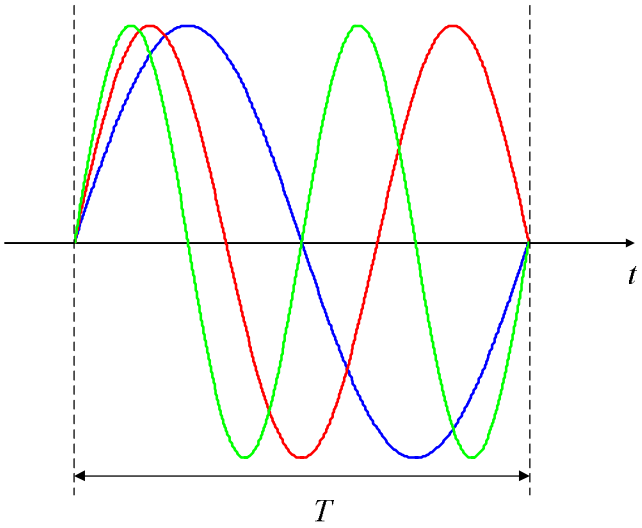

Fig. 1.1 Example of three orthogonal sub-carriers within one OFDM symbol

After passing through the IFFT, an OFDM signal is described by mathematical equation in eq.(1.1), where S_k is the complex value of k-th sub-carrier, N is the FFT point. Fig. 1.2 shows the data spectrum of eq. (1.1).

$$x(n) = \sum_{k=0}^{N-1} S_k \cdot e^{j\frac{2\pi kn}{N}} \tag{1.1}$$

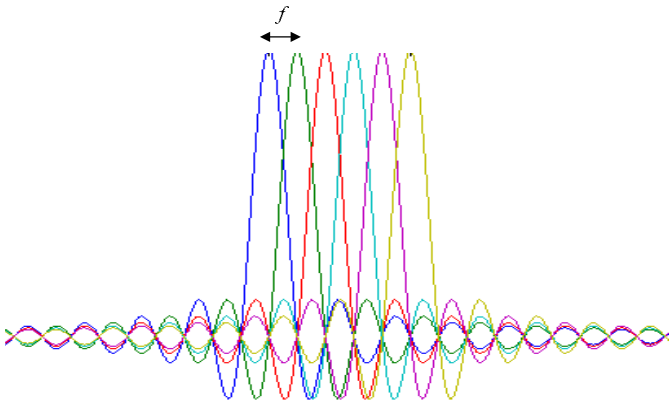

Fig. 1.2 Overlapped orthogonal sub-carriers

It can be seen from the above figure, which shows the overlapping SINC spectra of individual sub-carriers. At the maximum of each sub-carrier spectrum, all other sub-carrier spectra are zero. The frequency interval between any two adjacent sub-carriers is f. That is, the sub-carriers are overlapped to save bandwidth without ICI by using the orthogonal technique.

The other reason to use the OFDM technology is to avoid the Inter Symbol Interference (ISI) caused by multi-path effect. A cyclic prefix (CP), served as guard time, which is the copy of last N_g point, is introduced after IFFT in OFDM system. The length of guard time is chosen larger than the expected delay spread of multi-path channel to avoid ISI. As long as, the CP length is larger than the delay spread of channel, the linear convolution of signal and channel impulse response will result in circular convolution. Then, receiver can use only one-tap frequency domain equalizer to compensate the channel effect. The format of OFDM symbol in time domain can be shown in Fig. 1.3.

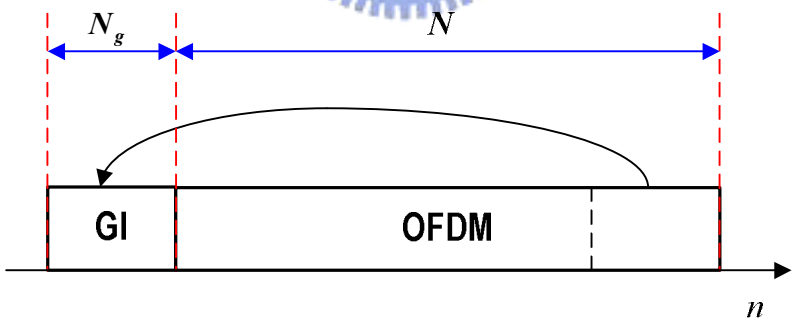

Fig. 1.3 OFDM Symbol

1.3. Introduction to Multi-Band OFDM Ultra Wide Band

Ultra Wide Band (UWB) [2] is a wireless personal network, which is built for in-home usage. They are envisioned to provide high-quality real-time video and audio distribution, file exchange among storage systems, and cable replacement for home entertainment systems. It offers high speed data transmission in short-range distance. It will be widely used in future digital home electronics industry.

1.3.1. UWB physical layer

The block diagram of the baseband transceiver is illustrated in Fig. 1.4. The system includes a 128 point FFT-based QPSK-OFDM modem, a soft-decision De-Mapper, a forward-error-correction (FEC) design, and an ideal timing synchronizer.

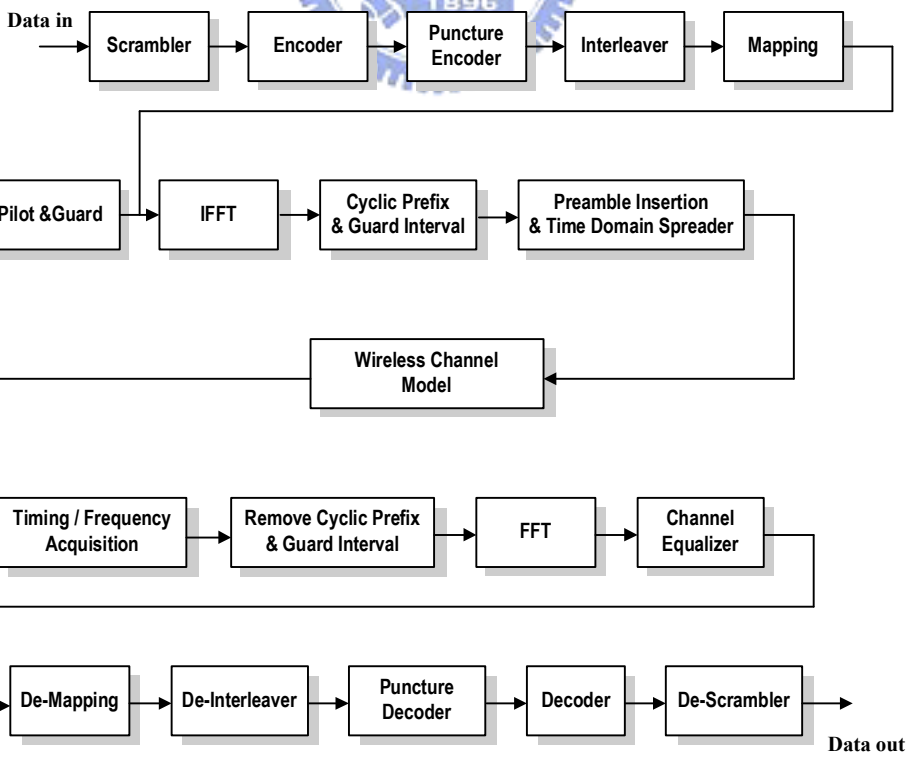

Fig. 1.4 Block Diagram of Baseband Transceiver

The UWB system utilizes the unlicensed 3.1 ~ 10.6 GHz band. UWB system provides data payload communication capabilities of 53.3, 55, 80, 106.67, 110, 160, 200, 320, and 480 Mb/s. The system uses a total of 122 sub-carriers that are modulated using quadrature phase shift keying (QPSK). Forward error correction coding (convolutional coding) is used with a coding rate of 1/3, 11/32, 1/2, 5/8, and 3/4. The system also utilizes a time-frequency code (TFC) to interleave coded data over 3 frequency bands. An example of this operation can be shown in Fig. 1.5. Table 1.1 shows the rate-dependent parameters in each data rate. In 53.3 Mb/s, 55 Mb/s and 80 Mb/s transmission modes, data sub-carriers are duplicated four times within an OFDM symbol. In 110 Mb/s, 160 Mb/s, 200 Mb/s modes, data sub-carriers are duplicated twice within an OFDM symbol.

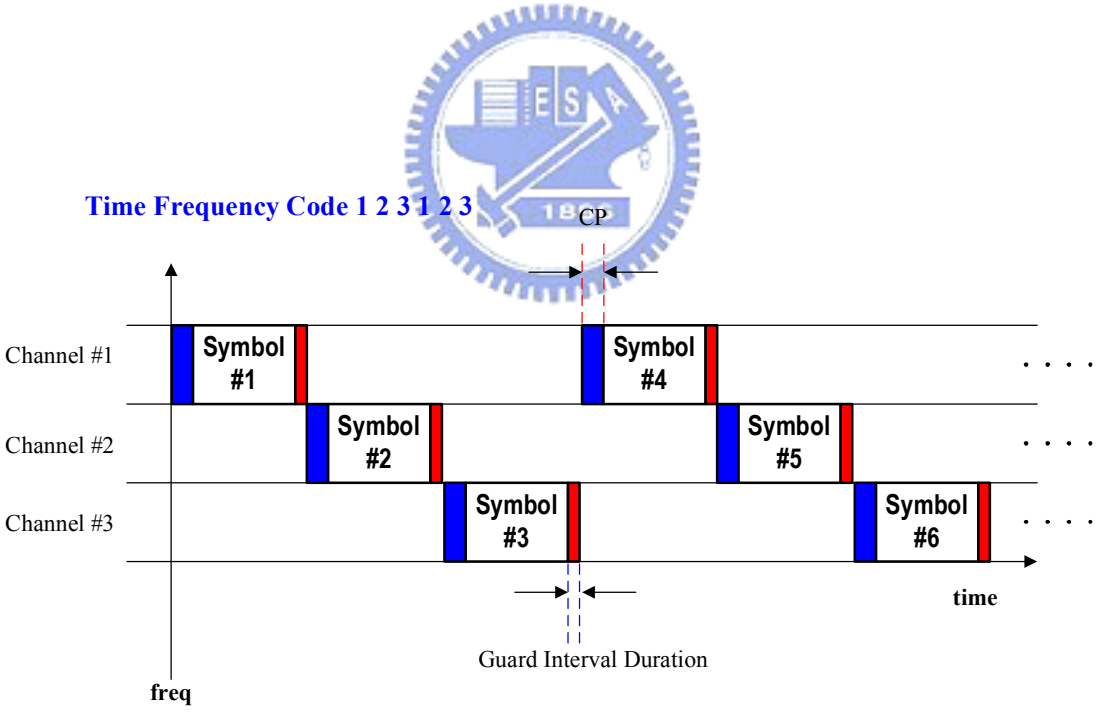

Fig. 1.5 TFC Example of UWB

Table 1.1 – Rate-dependent parameters for UWB

Data Rate (Mb/s)	Modulation	Coding rate (R)	Conjugate Symmetric Input to IFFT	Time Spreading Factor	Overall Spreading Gain	Coded bits per OFDM symbol (N_{CBPS})
53.3	QPSK	1/3	Yes	2	4	100
55	QPSK	11/32	Yes	2	4	100
80	QPSK	1/2	Yes	2	4	100
106.7	QPSK	1/3	No	2	2	200
110	QPSK	11/32	No	2	2	200
160	QPSK	1/3	No	2	2	200
200	QPSK	5/8	No	2	2	200
320	QPSK	1/2	No	1	1	200
400	QPSK	5/8	No	1 (No spreading)	1	200
480	QPSK	3/4	No	1 (No spreading)	1	200

In Table 1.2, it lists timing-related parameters. An OFDM symbol period is $T_{SYM} = T_{CP} + T_{FFT} + T_{GI} = 312.5$ ns. T_{CP} is the cyclic prefix which is used in OFDM to mitigate the effects of multi-path. The parameter T_{GI} is the guard interval duration. T_{FFT} is the 128-point FFT period which is 242.42 ns.

Table 1.2 – Timing-related parameters for UWB

Parameter	Value
N_{FFT} : Number of total sub-carriers	128
N_{SD}: Number of data sub-carriers	100
N_{SDP}: Number of defined pilot carriers	12
N_{SG}: Number of guard carriers	10
N_{ST}: Number of total sub-carriers used	122 (= $N_{SD} + N_{SDP} + N_{SG}$)
Δ_F: Sub-carrier frequency spacing	4.125 MHz (= 528 MHz/128)
T_{FFT}: IFFT/FFT period	242.42 ns ($1/\Delta_F$)
T_{CP}: Cyclic prefix duration	60.61 ns (= 32/528 MHz)
T_{GI}: Guard interval duration	9.47 ns (= 5/528 MHz)
T_{SYM}: Symbol interval	312.5 ns ($T_{CP} + T_{FFT} + T_{GI}$)

Fig. 1.6 shows the format for the PLCP frame. The PLCP frame includes PLCP preamble, PLCP header, frame payload, and inserted data. In PLCP preamble, 29 OFDM symbols are included. The packet synchronization sequences are used for packet detection and acquisition, coarse carrier frequency estimation, and coarse symbol timing. The frame synchronization sequences are used for synchronize the receiver algorithm. Finally, the channel estimation sequences {CE0, CE1, CE2, CE3, CE4, CE5} are used to estimate the channel frequency response, fine carrier frequency estimation, and fine symbol timing. In UWB specification, OFDM symbols are transmitted over three different sub-bands, so each sub-band can only use two channel estimation sequences.

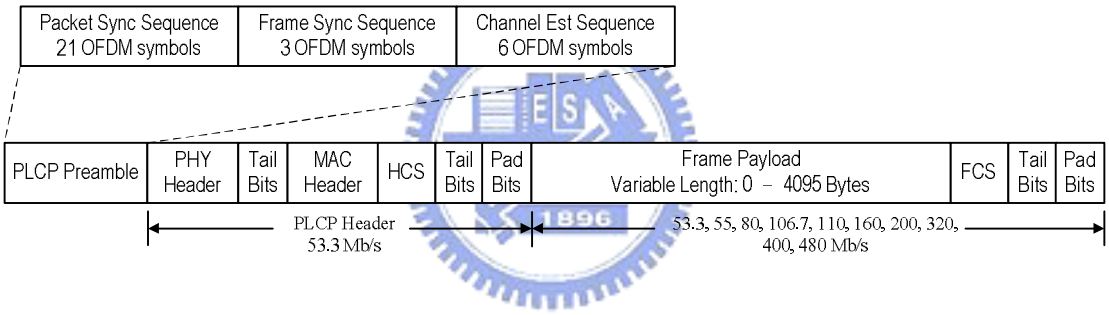

Fig. 1.6 UWB Frame Format

1.4. Introduction to IEEE 802.16d Fixed WIMAX

WIMAX [3] is a standard-based wireless technology that provides high-throughput broadband connections over long distances. WIMAX can be used for a number of applications, including "last mile" broadband connections, hot spots and high-speed data transmission. The advantages of high spectral efficiency, Low cost of deployment and good cell coverage make WIMAX a great candidate for metropolitan area wireless communication.

1.4.1. Fixed-WIMAX physical layer

The block diagram of the fixed-WIMAX is similar to UWB. Except to the Convolutional Code, WIMAX system adds the Reed-Solomon Code. The IFFT/FFT point is 256. There are multiple choices of bandwidth, and the maximum bandwidth is 28Mhz. Some of important parameters are listed in Table 1.3 and Table 1.4.

Table 1.3 –Timing related parameters for WIMAX

Parameter	Value
N_{FFT} : Number of total sub-carriers	256
N_{SD}: Number of data sub-carriers	192
N_{SDP}: Number of defined pilot carriers	8
N_{SG}: Number of guard carriers	55
N_{ST}: Number of total sub-carriers used	200 (= N_{SD} + N_{SDP})
Bandwidth	BW (1.5~28 MHz)
n: Sampling Factor	8/7
F_S: Sampling Frequency	Floor(n*BW/8000)*8000 (2~32 MHz)
Δ_F: Sub-carrier frequency spacing	F_S/N_{FFT}
G: Cyclic prefix to symbol time ratio	1/4, 1/8, 1/16, 1/32
T_B: Effective symbol time	$1/\Delta_F$
T_G: Guard interval time	G* T_B

Table 1.4 –Available bandwidth list for WIMAX

BW (*MHz*)		T_B (*us*)	$T_G = T_B/32$ (*us*)	$T_G = T_B/16$ (*us*)	$T_G = T_B/8$ (*us*)	$T_G = T_B/4$ (*us*)
n=8/7	1.75	128	4	8	16	32
	3.5	64	2	4	8	16
	7.0	32	1	2	4	8
	14.0	16	0.5	1	2	4
	28.0	8	0.25	0.5	1	2

In fixed-WIMAX, there are seven different transmission types defined IEEE 802.16d standard. They are shown in Table 1.5.

Table 1.5 –Seven different transmission types for WIMAX

Modulation	Uncoded block size (bytes)	Coded block size (bytes)	Overall Coding rate	RS code	CC code rate
BPSK	12	24	1/2	(12,12,0)	1/2
QPSK	24	48	1/2	(32,24,4)	2/3
QPSK	36	48	3/4	(40,36,2)	5/6
16-QAM	48	96	1/2	(64,48,8)	2/3
16-QAM	72	96	3/4	(80,72,4)	5/6
64-QAM	96	144	2/3	(108,96,6)	3/4
64-QAM	108	144	3/4	(120,108,6)	5/6

In IEEE 802.16d standard, the frame consists of a downlink sub-frame and an uplink sub-frame. With different duplexing methods, there are two frame structures. In this thesis, Frequency Division Duplex (FDD) is used to transmit the signal. Fig. 1.7 shows the FDD frame structure. The downlink PHY PDU starts with a long preamble. The preamble is followed by a FCH burst. FCH burst is one OFDM

symbol long and is transmitted using BPSK rate 1/2. It specifies burst profile and length of one or several downlink bursts immediately following the FCH. After FCH, data bursts are transmitted.

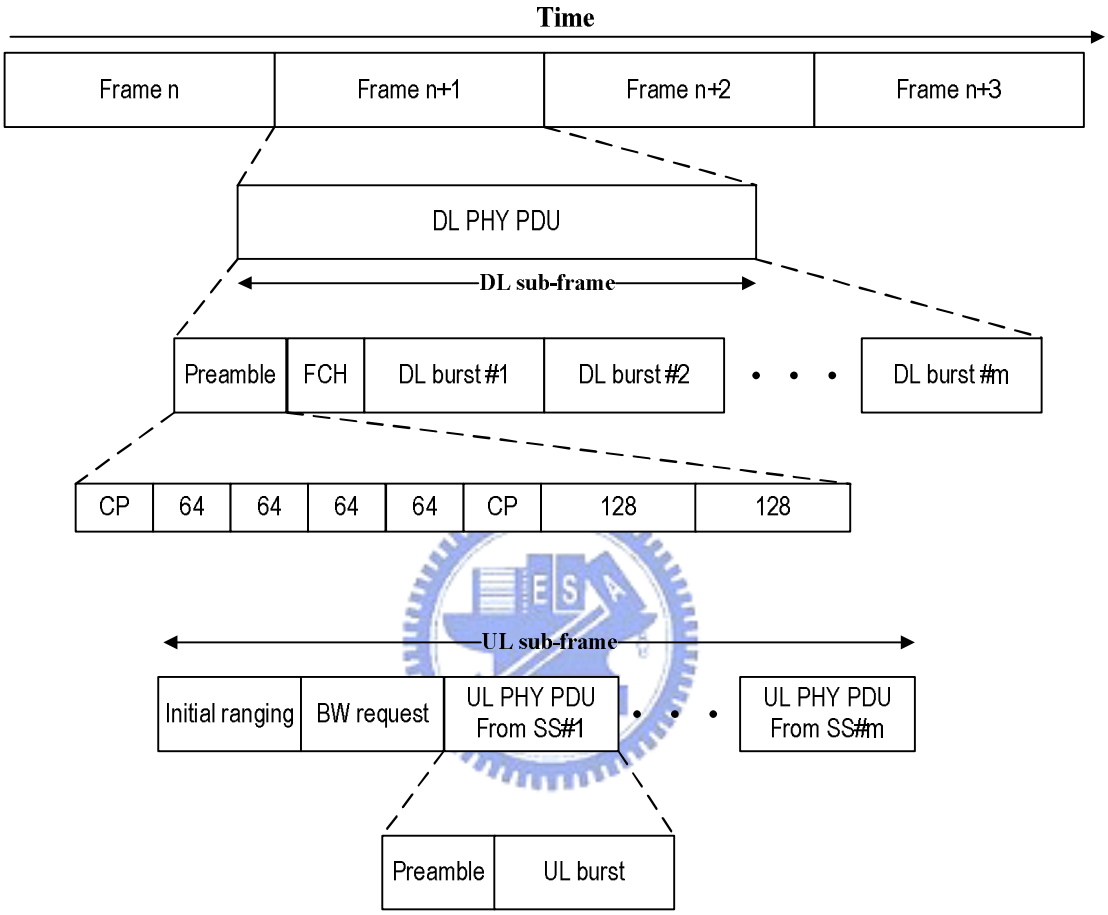

Fig. 1.7 WIMAX Frame Format

1.5. Channel Equalizer Design Spec

In OFDM system, the multi-path channel, AWGN, Carrier frequency Offset (CFO) between transmitter and receiver, and Sampling Clock Offset (SCO) between DAC and ADC, are the four main data distortion issues. In order to solve the multi-path channel effect, preambles are used to estimate the fading channel. Then, receiver uses the estimated channel to do the equalization. Because of the existence of AWGN, it will cause channel estimation (CE) error. This CE error will be propagated to the equalizer and leads to performance degradation. The way to lower down the CE error will be introduced in chapter 3.

Residual CFO and SCO will cause phase rotation in frequency domain, and result in ICI. Phase Error Tracker (PET) is applied in OFDM systems for phase rotation tracking and compensation. The detail algorithm for PET will also be introduced in chapter 3.

Chapter 2.
Design Specification of Dual-Mode Channel Equalizer

2.1. Wireless Channel Model

In order to simulate the practical data transmission, the wireless channel model must be established. The channel model comprises multi-path fading channel, CFO, SCO, AWGN. The details are introduced individually below.

2.2. Intel Proposed UWB Multi-paths Channel Model

The Intel proposed channel model [4] is based on the observation that usually multi-path contributions generated by the same pulse arrive at the receiver grouped into clusters. The time of arrival of clusters is modeled as a Poisson arrival process with rate Λ:

$$p(T_n \mid T_{n-1}) = \Lambda e^{-\Lambda(T_n - T_{n-1})} \tag{2.3}$$

Where T_n and T_{n-1} are the times of arrival of the *n*-th and the (*n-1*)-th clusters.

Within each cluster, subsequent multi-path contributions also arrive according to a Poisson process with rate λ:

$$p(\tau_{nk} \mid \tau_{(n-1)k}) = \lambda e^{-\lambda(\tau_{nk} - \tau_{(n-1)k})} \tag{2.4}$$

Where τ_{nk} and $\tau_{(n-1)k}$ are the time of arrival of the *n*-th and the (*n-1*)-th contributions

within cluster *k*.

The channel impulse response of the IEEE model can be expressed as follow:

$$h(t) = X \sum_{n=1}^{N} \sum_{k=1}^{K(n)} \alpha_{nk} \delta(t - T_n - \tau_{nk}) \tag{2.1}$$

where X is a log-normal random variable representing the amplitude gain of the channel. N is the number of observed clusters. $K(n)$ is the number of multi-path contributions received within the *n*-th cluster. α_{nk} is the coefficient of the *k*-th multi-path contribution of the *n*-th cluster. T_n is the time of arrival of the *n*-th cluster, and τ_{nk} is the delay of the *k*-th multi-path contribution within the *n*-th cluster.

The channel coefficient α_{nk} can be defined as follows:

$$\alpha_{nk} = p_{nk} \beta_{nk} \tag{2.2}$$

where p_{nk} is discrete random variable assuming values ±1 with equal probability and β_{nk} is the log-normal distributed channel coefficient of multi-path contribution *k* belonging to cluster *n*. The β_{nk} term can be expressed as follows:

$$\beta_{nk} = 10^{\frac{x_{nk}}{20}} \tag{2.3}$$

Where x_{nk} is assumed to be a Guassian random variable with mean μ_{nk} and the

standard deviation σ_{nk}.

Variable x_{nk} in particular, can be future decomposed as follows:

$$x_{nk} = \mu_{nk} + \xi_n + \zeta_{nk} \tag{2.4}$$

where ζ_n and ξ_{nk} are two Gaussian random variables that represent the fluctations of the channel coefficient on each cluster and on each contribution. We indicate the variance of ζ_n and ξ_{nk} by σ_ζ^2 and σ_ξ^2. The μ_{nk} value is determined to reproduce the exponential power decay for the amplitude of the multi-path contribution with in each cluster. One can write:

$$\left\langle \left|\beta_{nk}\right|^2 \right\rangle = \left\langle \left| 10^{\frac{\mu_{nk}+\xi_{nk}+\zeta_{nk}}{20}} \right|^2 \right\rangle = \left\langle \left|\beta_{00}\right|^2 \right\rangle e^{-\frac{T_n}{\Gamma}} e^{-\frac{\tau_n}{\gamma}}$$
$$\Rightarrow \mu_{nk} = \frac{10\ln\left(\left\langle \left|\beta_{00}\right|^2 \right\rangle\right) - 10\frac{T_n}{\Gamma} - 10\frac{\tau_n}{\gamma}}{\ln(10)} - \frac{\left(\sigma_\xi^2 + \sigma_\zeta^2\right)\ln(10)}{20} \tag{2.5}$$

The total energy contained in the β_{nk} terms must be normalized to unity for each realization, this is:

$$\sum_{n=1}^{N}\sum_{k=1}^{K(n)} \left|\beta_{nk}\right|^2 = 1 \tag{2.6}$$

The amplitude gain X in eq. 2.1 is assumed to be a log-normal random variable:

$$X = 10^{\frac{g}{20}} \tag{2.7}$$

Where g is Gaussian random variable with mean g_0 and variance σ_g^2 . The g_0 value depends on the average total multi-path gain G.

$$g_0 = \frac{10\ln(G)}{\ln(10)} - \frac{\sigma_g^2 \ln(10)}{20} \tag{2.8}$$

The value can be determined as indicated below:

$$G = \frac{G_0}{D^{\gamma}}$$
$$G_0 = 10^{-A_0/10} \tag{2.9}$$

In eq. 2.8, A_0 (in dB) = $10\log(E_{TX}/E_{RX0})$. Values for both A_0 and γ are suggested in (Ghassemzadeh and Tarokh, 2003) for different propagation environments: A_0=47dB and γ=1.7 for a LOS environment, and A_0= 51dB and γ=3.5 for a NLOS environment.

According to the above definitions, the channel model represented by the impulse response is fully characterized when the following parameters are defined:

- Λ : The cluster average arrival rate
- λ : The ray average arrival rate
- Γ : The power decay factor for clusters
- γ : The power decay factor for rays in a cluster
- σ_{ξ} : The standard deviation of the fluctuations of the channel coefficients for clusters

- σ_ζ : The standard deviation of the fluctuations of the channel coefficients for rays in each cluster
- σ_g : The standard deviation of the channel amplitude gain

The IEEE suggested an initial set of values for the above parameters. These values will shows in Table 2.1.

Table 2.1 –Parameter Settings for the IEEE UWB Channel Model

Scenario	Λ	λ	Γ	γ	σ_ξ	σ_ζ	σ_g
Case A (CM1) LOS (0-4 m)	0.0233	2.5	7.1	4.3	3.3941	3.3941	3
Case B (CM2) NLOS (0-4 m)	0.4	0.5	5.5	6.7	3.3941	3.3941	3
Case C (CM3) NLOS (4-10 m)	0.0667	2.1	14	7.9	3.3941	3.3941	3
Case D (CM4) Extreme NLOS Multi-path Channel	0.0667	2.1	24	12	3.3941	3.3941	3

The channel impulse response (CIR) and the corresponding channel frequency response (CFR) of CM2, CM4 are shown in Fig. 2.1.

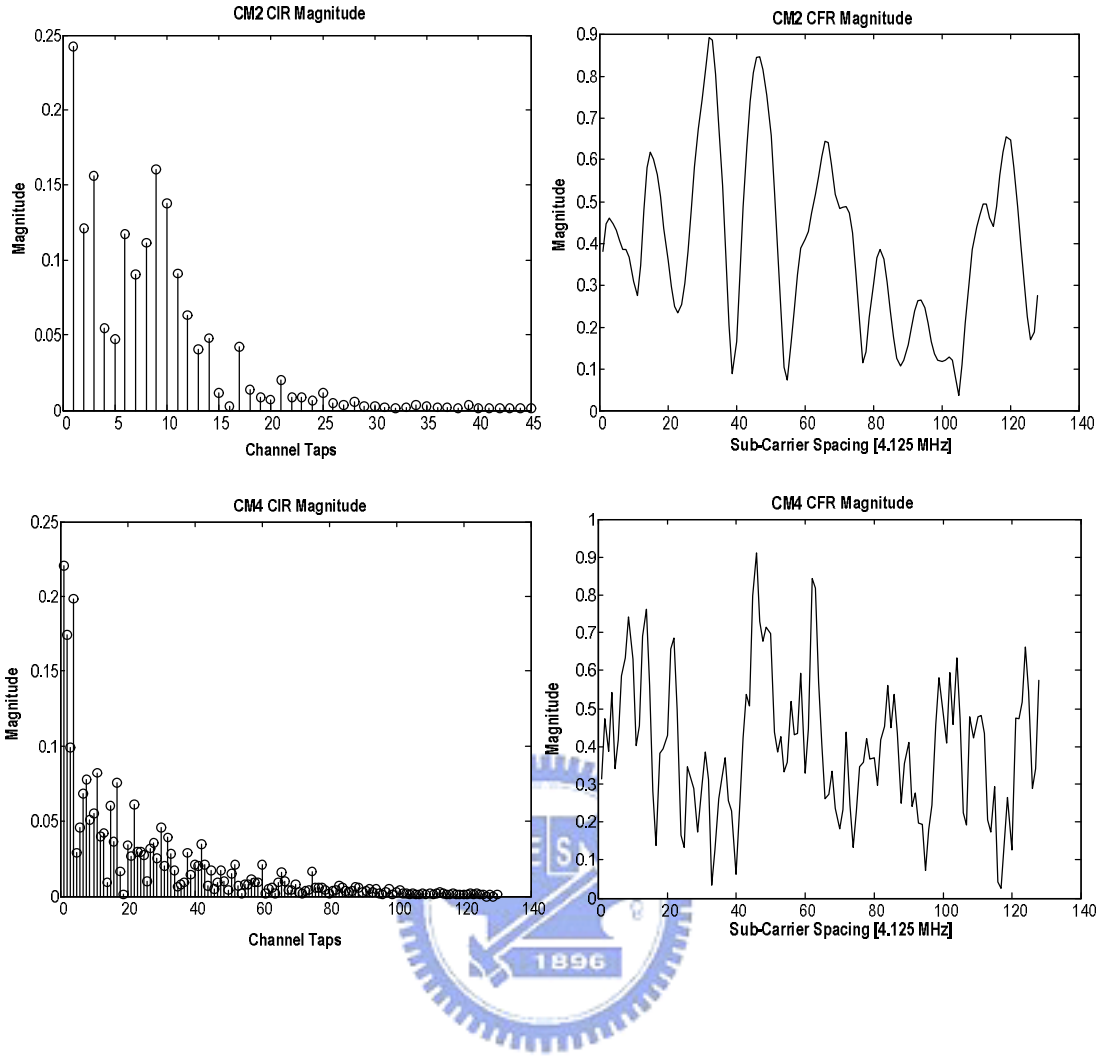

Fig. 2.1 CIR, CFR of the CM2 and CM4

2.3. *WIMAX SUI Channel Model*

In 802.16d system, a series of Stanford University Interim (SUI) [5] channel with three terrain types are selected for application on fixed broadband wireless. According to the different terrain and tree density, the six SUI channels can be classified into three categories as showed in Table 2.2

Table 2.2 –SUI Channel

Model	**Category**
SUI1	Flat terrain with light tree densities
SUI2	
SUI3	Hilly terrain with light tree densities
SUI4	
SUI5	Hilly terrain with moderate-to-heavy tree densities
SUI6	

The narrow band received signal fading can be characterized by a Ricean distribution. The key parameter of this distribution is the K-factor, defined as the ratio of the "fixed" component power and the "scatter" component power. The narowband K-factor distribution was found to be lognormal, with the median as a simple function of season, antenna height, antenna beamwidth, and distance. The standard deviation was found to be approximately 8 dB. K-factor model is presented as follows:

$$K = F_S F_h F_b K_0 d^{\gamma} u \tag{2.10}$$

Where F_S is a seasonal factor, F_S =1.0 in summer (leaves):2.5 in winter (no leaves)

F_h is the receive antenna height factor, $F_h = (h/3)^{0.46}$ (h is the receive antenna heigh in meters)

F_b is the beamwidth factor, $F_b = (b/17)^{-0.62}$ (b in degrees)

K_0 and γ are regression coefficients, K_0= 10; γ = -0.5

u is a lognormal variable which has zero dB mean and standard deviation of 8.0 dB

We use the method of filtered noise to generate channel coefficients with the specified distribution and spectral power density. For each tap a set of complex zero-mean Gaussian distributed numbers is generated with a variance of 0.5 for the real and imaginary part. Total average power of this distribution is 1. This yields a normalized Rayleigh distribution for the magnitude of the complex coefficients. For the Ricean distribution (K>0), a constant path component m has to be added to the Rayleigh set of coefficients. The ratio of powers between this constant part and the Rayleigh (variable) part is specified by the K-factor. The following equation shows the distribution of the power by stating the total power p of each tap.

$$\begin{aligned} P &= |m|^2 + \sigma^2 \\ K &= \frac{|m|^2}{\sigma^2} \\ \sigma^2 &= P\frac{1}{K+1} \; and \; |m|^2 = P\frac{K}{K+1} \end{aligned} \tag{2.11}$$

Where m is the complex constant and σ^2 is the variance of the complex Gaussian set. The generated coefficients of channel taps have a white spectrum since they are independent of each other. The SUI channel model defines a specific power spectral

density (PSD) function for these scatter component channel coefficients is given as:

$$S(f) = \begin{cases} 1 - 1.72 f_0^2 + 0.785 f_0^4 & , |f_0| \le 1 \\ 0 & , |f_0| > 1 \end{cases} \quad where\ f_0 = \frac{f}{f_m} \tag{2.12}$$

To arrive at a set of channel coefficients with this PSD function, we correlate the original coefficients with a filter which amplitude frequency response is derived from eq. 2.12 as

$$|H(f)| = \sqrt{S(f)} \tag{2.13}$$

Without changing the total power of transmitted signal, the total power of the Doppler filter has to be normalized to one. Consequently, after passing through the Doppler filter, normalized factor is applied to normalize these multi-path fading taps. Table 2.3 shows the parameters of six SUI channels. Table 2.4 shows the normalization factor for each SUI channel.

Table 2.3 -SUI Channel Parameters

Model	RMS delay (us)	Parameter	Tap1	Tap2	Tap3	K-factor
SUI-1	0.111	Delay(us)	0	0.4	0.9	[4 0 0]
		Power(dB)	0	-15	-20	
		Doppler Frequency (Hz)	0.4	0.3	0.5	
SUI-2	0.202	Delay(us)	0	0.4	1.1	[2 0 0]
		Power(dB)	0	-12	-15	
		Doppler Frequency (Hz)	0.2	0.15	0.25	
SUI-3	0.264	Delay(us)	0	0.4	0.9	[1 0 0]
		Power(dB)	0	-5	-10	
		Doppler Frequency (Hz)	0.4	0.3	0.5	

SUI-4	1.257	Delay(us)	0	1.5	4	[0 0 0]
		Power(dB)	0	-4	-8	
		Doppler Frequency (Hz)	0.2	0.15	0.25	
SUI-5	2.842	Delay(us)	0	4	10	[0 0 0]
		Power(dB)	0	-5	-10	
		Doppler Frequency (Hz)	2	1.5	2.5	
SUI-6	5.240	Delay(us)	0	14	20	[0 0 0]
		Power(dB)	0	-10	-14	
		Doppler Frequency (Hz)	0.4	0.3	0.5	

Table 2.4 -Normalization Factors

SUI Channel Models	Normalization Factor (dB)
SUI-1	-0.1771
SUI-2	-0.3930
SUI-3	-1.5113
SUI-4	-1.9218
SUI-5	-1.5113
SUI-6	-0.5683

For system bandwidth equal to 20MHz, the examples of CIR and CFR for SUI-1 to SUI-3 are shown in Fig. 2.2 to Fig. 2.4.

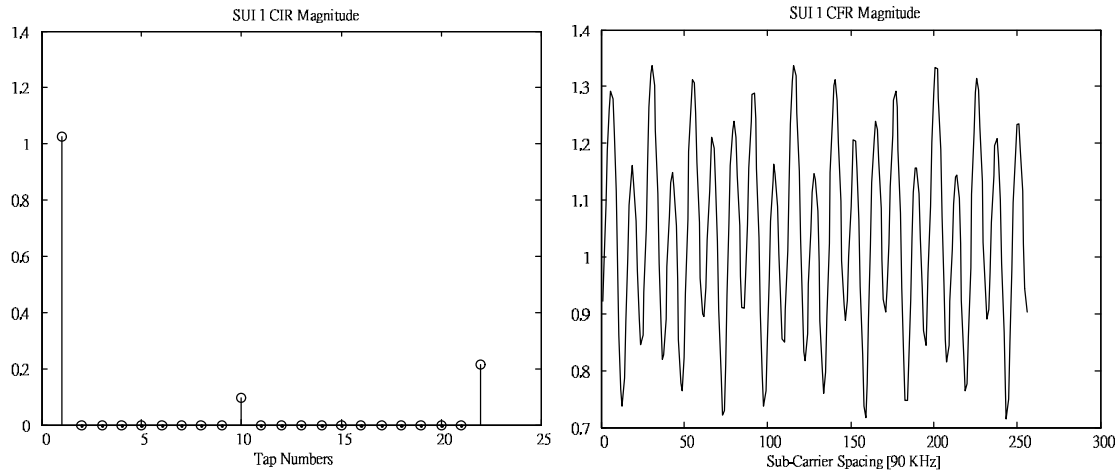

Fig. 2.2 CIR and CFR for SUI-1

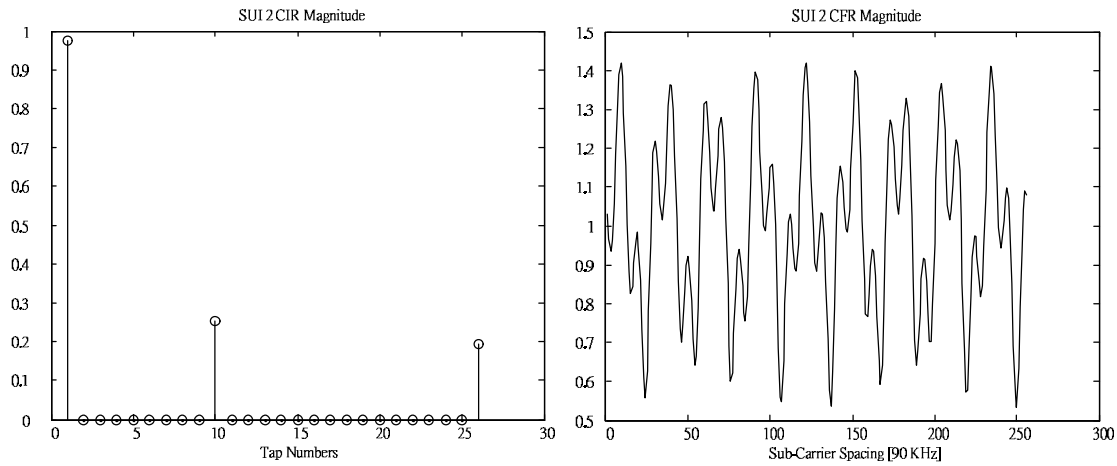

Fig. 2.3 CIR and CFR for SUI-2

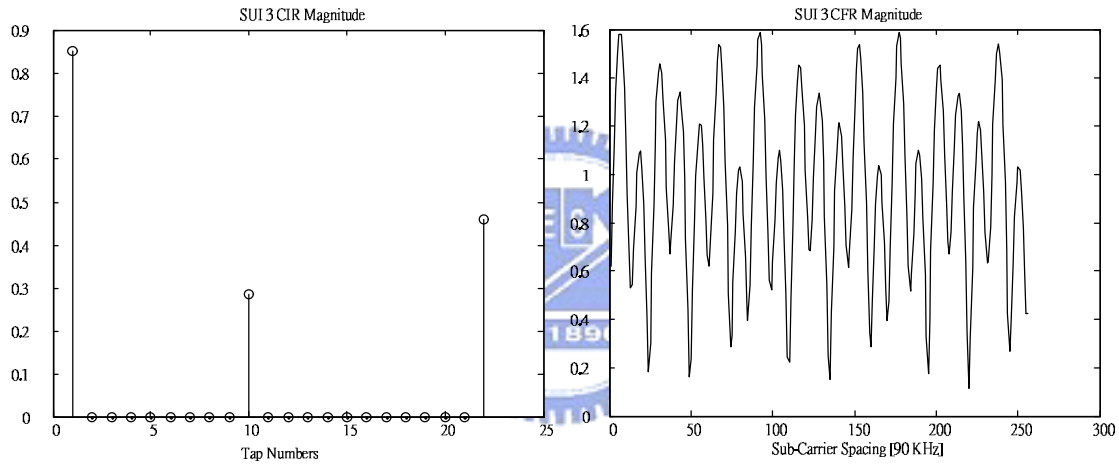

Fig. 2.4 CIR and CFR for SUI-3

2.4. *Carrier Frequency Offset Model*

Carrier Frequency Offset (CFO) [1] is caused by the mismatch in RF local frequency between transmitter and receiver. When CFO is existed in transmission path, the received sub-carrier will be influence by the other sub-carriers, which is referred as ICI. ICI effect caused by CFO is shown in Fig. 2.5.

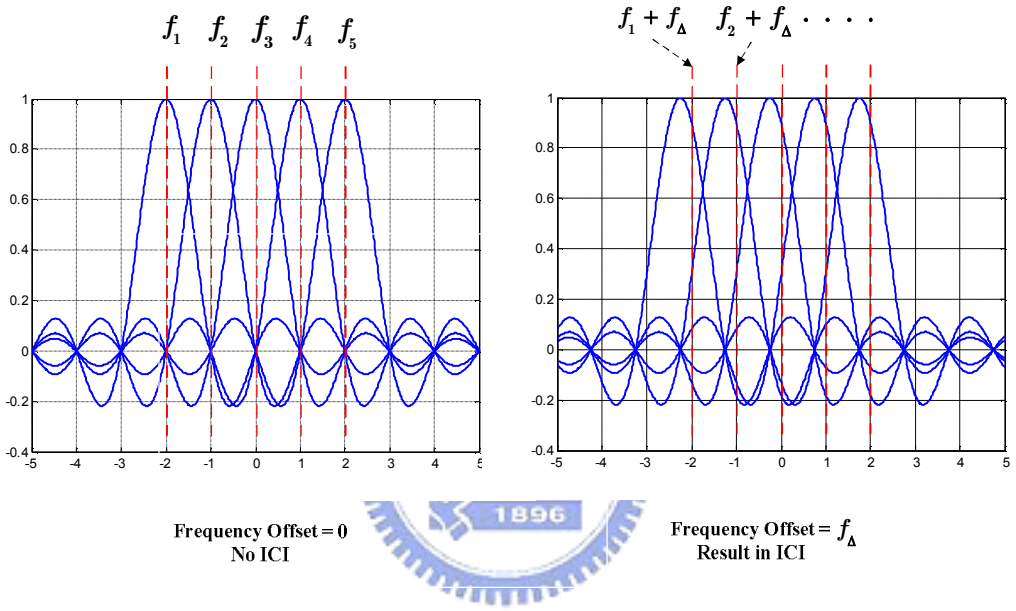

Fig. 2.5 ICI effect

Assuming the transmitted signal is $S(t)$, transmitted carrier frequency is f_c, received carrier frequency is $f_c + \varepsilon\Delta f$, Δf is the sub-carrier spacing, and ε is the frequency offset. The received signal after down conversion is given as:

$$R(t) = S(t) \cdot e^{j2\pi f_c t} \cdot e^{-j2\pi(f_c+\Delta f)t} = S(t) \cdot e^{-j2\pi\Delta f \cdot t} \tag{2.12}$$

Finally, CFO effect is simulated by multiplying the original signal with a phase rotation. This phase rotation is increased by the time as it can be seen from eq. 2.12.

2.5. *Sampling Clock Offset Model*

SCO is caused by ADC/DAC sampling frequency mismatch. Because of SCO, the sampling points will slowly shift with time. This shift in time domain will result in phase rotation in frequency domain and ICI. Fig. 2.6 shows the concept of SCO, where T_s is the sampling time and μ is the value of timing offset.

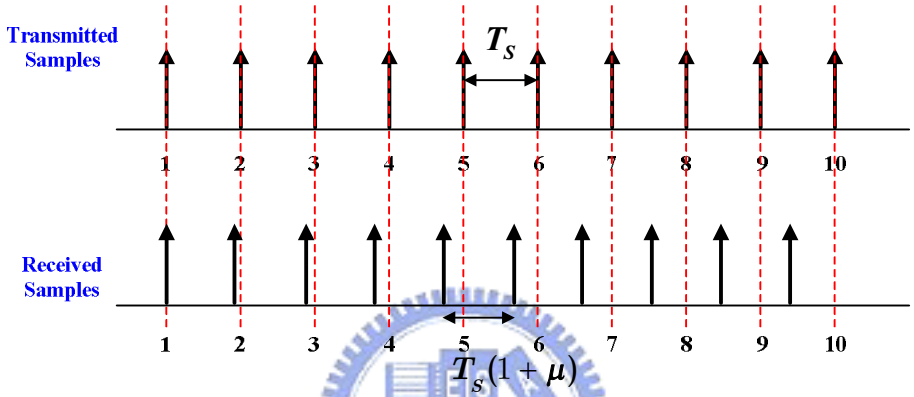

Fig. 2.6 SCO effect

The SCO model is established by the concept of interpolation with 20 taps raised cosine filter [6]. The FIR filter structure of the interpolator is shown in Fig. 2.7. This filter performs a linear combination of (I_1+I_2+1=20) signal samples $x(nT_S)$ taken around the basepoint m_k, and the operation can be shown in eq. 2.13. In eq. 2.13, $h_i(\mu)$ is the coefficient of FIR filter tap, the sampled value of the raised cosine function. The corresponding sampled value is shown in eq. 2.14 and Fig. 2.8.

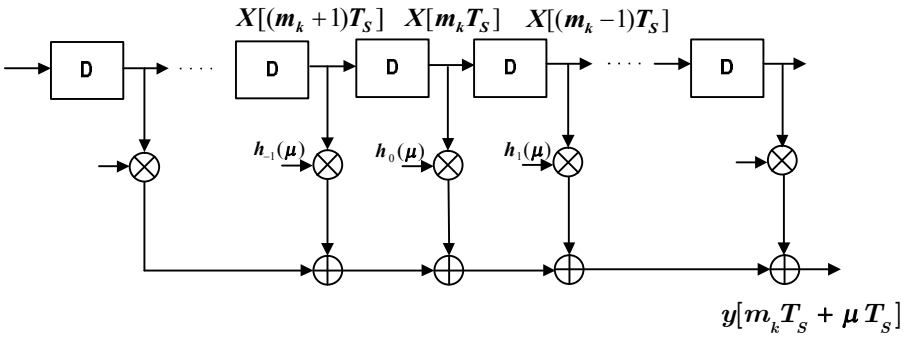

Fig. 2.7 FIR filter structure

$$y(m_k T_s + \mu T_s) = \sum_{i=I_1}^{i=I_2} x\left[\left(m_k - i\right)T_s\right] h_i(\mu) \tag{2.13}$$

$$h_i(\mu) = \frac{\cos[\pi\beta(i+\mu)]}{1-4\beta^2(i+\mu)^2}\sin c(i+\mu) \tag{2.14}$$

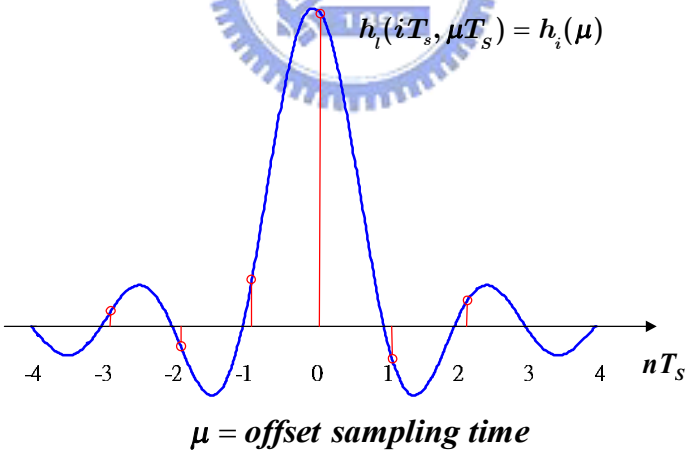

Fig. 2.8 Sampled value of the raised cosine function

2.6. Additive White Gaussian Noise

The AWGN is established by the random generator ($randn$). The output random signal is normally distributed with zero mean and variance equal to 1. The AWGN noise can be modeled as

$$w = [randn(1,n) + j \cdot randn(1,n)] \cdot \sqrt{\frac{10^{\frac{P_S - SNR}{10}}}{2}} \tag{2.15}$$

Where P_S is signal power, SNR is signal-to-noise ratio (dB), and n is length of data signal.

Chapter 3.
Design of Dual-Mode Channel Equalizer

In this chapter, a low complexity and high performance dual-mode channel equalizer is proposed. It includes channel estimator, equalizer, phase error tracker and modified normalized least-mean-square (NLMS) channel tracker. Data distortion caused by multi-path fading, AWGN, residual CFO and SCO can be eliminated by these four parts. Following is the block diagram of the proposed channel equalizer. After passing through the FFT, channel estimator uses received preambles to estimate the channel frequency response (CFR). The estimated CFR will be sent to the equalizer. Then, equalizer uses the estimated CFR to equalize the distorted data sub-carriers. After doing the equalization, equalized data sub-carriers will be sent to the phase error tracker and compensator. The tracked phase error combined with unequalized data, equalized data and estimated CFR are then sent to modified NLMS channel tracker to calculate the updated CFR. Finally, compensated data sub-carriers are sent to De-Mapper.

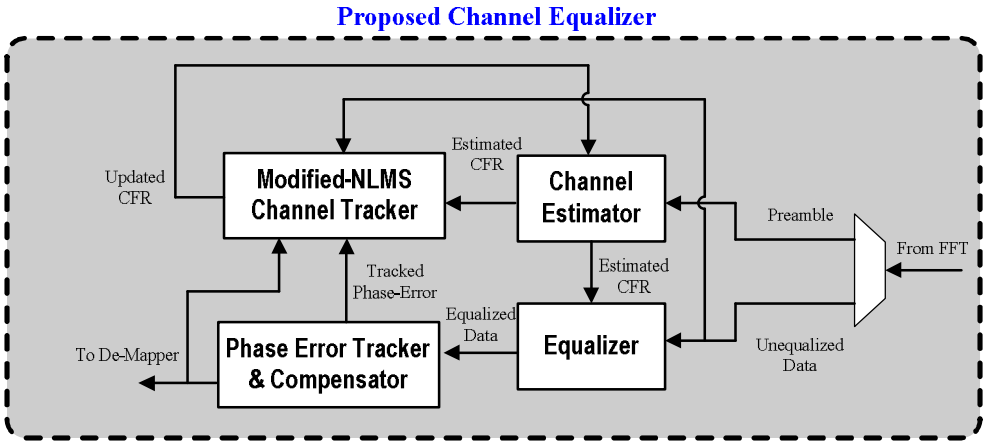

Fig. 3.1 Block Diagram of Proposed Channel Equalizer

3.1. Dual-Mode Design of Channel Estimation

The signal is transmitted over frequency-selective fading channel. After removing the cyclic prefix and guard interval, the post-FFT signal of the *l*-th OFDM symbol can be expressed by:

$$Y_l(k) = \sum_{n=0}^{N-1} z_{l,n} \cdot e^{-j2\pi\,(n/N)\,k} \tag{3.1}$$

where $z_{l,n}$ is the time domain data, N is the number of FFT points. Under consideration of CFO Δf, SCO $\zeta = (T' - T)/T$, and symbol timing offset n_ε, the post-FFT signal can be simplified as an equivalent model [7]:

$$Y_l(k) = \alpha(\phi_k)\alpha(n_\varepsilon)X_l(k)H_k e^{[j2\pi(k/N)n_\varepsilon]} \cdot e^{[j2\pi l\phi_k(T_u+T_g)/T_u]} + W_{l,k} \tag{3.2}$$

where $\phi_k = \Delta f T_u + \zeta \cdot k$, $\alpha(n_\varepsilon), \alpha(\phi_k)$ are the attenuation factors, $X_l(k)$ is the transmitted data at the *k*-th sub-carrier, T_u is the duration of FFT, T_g is the guard interval, T is the sampling time, T' is the offset sampling time, $W_{l,k}$ is the noise caused by AWGN, symbol timing offset, ICI, and other non-ideal parameters. With the assumption that the timing synchronization is perfect, there is no timing offset. The equivalent model can be simplified as:

$$Y_l(k) = \alpha(\phi_k)\; X_l(k)\, H_k\, e^{[j2\pi\, l\, \phi_k (T_u+T_g)/T_u]} + W_{l,k} \tag{3.3}$$

Where the attenuation factor $\alpha(\phi_k)$ is very close to 1 and therefore can be neglected.

3.1.1. Channel Estimation for UWB

In UWB system, use zero-forcing (ZF) methodology with received two preambles to estimate the fading channel. Using the average value, the estimation error can be reduced and the performance will be improved. Simulation result shows that it will contribute 1~2dB gain in SNR. Considering that the pre-defined signal $X_L(k)$ in preamble, the estimated of the *k*-th sub-channel is given by:

$$H_E(k) = \left(Y_{L1}(k) + Y_{L2}(k)\right) / 2X_L(k) \tag{3.4}$$

Where $Y_{L1}(k)$, $Y_{L2}(k)$ are the first and second received preamble.

In channel estimation, these two received preambles are also used to estimate the noise power which can be described as follows:

$$\begin{aligned} &\frac{1}{N}\sum_{k=0}^{N-1}\left|Y_{L1}(k)-Y_{L2}(k)\right|^2 \approx \frac{1}{N}\sum_{k=0}^{N-1}\left|\triangle W(k)\right|^2 \approx 2\sigma_E^2 \\ &\rightarrow \sigma_E^2 = \frac{1}{2N}\sum_{k=0}^{N-1}\left|Y_{L1}(k)-Y_{L2}(k)\right|^2 \end{aligned} \tag{3.5}$$

Where $\Delta W(k)$ is the white noise, σ_E^2 is the estimated noise power.

Based on the correlative property between adjacent sub-channels, the estimation of sub-channels can be further improved by delivering them into the 3-taps smoothing filter. The smoothing filter is a finite impulse response filter [8], which can be described as:

$$S(k) = \frac{\sum_{m=-1}^{1} c_m \cdot \delta(k-m)}{\sum_{m=-1}^{1} c_m} \tag{3.6}$$

After doing channel estimation, the estimated sub-channel $H_E(k)$ will be convoluted by the smoothing filter. The equation is given by:

$$H_S(k) = \sum_{m=-1}^{1} H_E(k-m) \cdot S(m) \tag{3.7}$$

After smoothing, each sub-channel will be a weighted summation of itself and nearby sub-channels. Simulation reveals that the system performance on PER will improve about 1dB for different transmission modes.

3.1.2. Channel Estimation for WIMAX

In WIMAX system, long preamble is used to estimate the fading channel. In standard of 802.16-2004, only even sub-carriers are utilized in long preamble. DC sub-carrier and odd sub-carriers are transmitted with zero value. Consequently, the ZF methodology is used to estimate the CFR of even sub-carriers at first, and then use 6-tap raised-cosine interpolator to get CFR of DC sub-carrier and odd sub-carriers. Following is the description of channel estimation for WIMAX system.

Considering that the pre-defined signal $X_L(k)$ in preamble, the estimated CFR of the *k*-th even sub-carrier is given by:

$$H_{E,even}(k) = Y_L(k) \;/\; X_L(k) \tag{3.8}$$

Where $Y_L(k)$ is the received long preamble.

Then, the 6-tap raised-cosine interpolator [6] is used to interpolate the CFR of odd sub-carriers and DC sub-carrier. Following is the impulse response of 6-tap

raised-cosine interpolator:

$$W(k) = \frac{\sin(\pi k / D)}{\pi k / D} \cdot \frac{\cos(\pi \beta k / D)}{1 - 4\beta^2 k^2 / D^2} \tag{3.9}$$

Where D is the spacing of even sub-carriers, and β is the roll-off factor. And, let k equal to -5, -3, -1, 1, 3, 5, the coefficient of six taps can be generated.

But, using 6-tap raised-cosine interpolator to get CFR of sub-carrier number -99, -97, 97, 99 will result in large error [9]. For example, to get CFR of sub-carrier number -99, it needs CFR of sub-carrier number -104, -102, -100, -98, -96, -94. But, sub-carriers are transmitted with zero value at number -104, -102. Receiver doesn't have any information at these two places. If zero value is applied to substitute the CFR of these two places, it will result in large error. So, the linear interpolation is used to get the CFR of sub-carrier number -99, -97, 97, 99.

Otherwise, DC sub-carrier (number 0) is transmitted with zero value. In order to get CFR of sub-carrier number -5, -3, -1, 1, 3, 5, CFR of DC sub-carrier is needed. To interpolate the DC value, CFR of sub-carrier number -10, -6, -2, 2, 6, 10 are used to get the CFR of DC sub-carrier [9]. Next, DC value is used to get the CFR of sub-carrier number -5, -3, -1, 1, 3, 5. For example, to interpolate the CFR of sub-carrier number 5, CFR of sub-carrier number DC, 2, 4, 6, 8, 10 are used as inputs to the interpolator. Following the same rule, CFR of sub-carrier number -5, -3, -1, 1, 3 can be generated.

According to the above statement, 6-tap raised-cosine interpolator is needed. Using 6-tap raised-cosine interpolator to get CFR of odd sub-carrier can be described as follows:

$$H_{E,odd}(k) = \sum_{m=-3}^{2} H_{k+mD+1} \cdot \frac{\sin(\pi(mD+1)/D)}{\pi(mD+1)/D} \cdot \frac{\cos(\pi\alpha(mD+1)/D)}{1-4\alpha^2((mD+1)/D)^2} \quad (3.10)$$

Using ZF channel estimation with 6-tap raised-cosine interpolator, the whole CFR can be generated.

3.2. Dual-Mode Design of Equalization

For UWB system, the modulation type is QPSK. Minimum mean square error (MMSE) methodology is very suitable to equalize the distorted signal. Traditional zero-forcing equalization will increase the noise and degrade the system's performance. Consequently, MMSE equalization is used to suppress the interference and noise effects in UWB system. The compensating value of the MMSE equalization can be derived as:

$$C_{MMSE}(k) = \frac{H_S(k)^*}{\left|H_S(k)\right|^2 + \dfrac{\sigma_E^2}{\left|X_L(k)\right|^2}} \quad (3.11)$$

Where $H_s(k)$ is the smoothed CFR, and σ_E^2 is estimated noise power from channel estimation part, $\left|X_L(k)\right|^2$ is transmitted preamble power, which can be fixed as 1 in UWB system. Finally, the signal is equalized as:

$$\hat{X}_l(k) = Y_l(k) \cdot C_{MMSE}(k) \quad (3.12)$$

For WIMAX system, there are four different modulation types, such as BPSK, QPSK, 16-QAM, 64-QAM. For 16-QAM, 64-QAM conditions, using MMSE

methodology to do equalization will suppress the signal and noise simultaneously. The attenuation signal will cross the decision boundary, and result in decision error. Consequently, MMSE methodology is not suitable for WIMAX system. In this place, ZF methodology is used to equalize the distorted signal. Following is the compensating value of the ZF equalization:

$$C_{ZF}(k) = 1 / H_E(k) \tag{3.13}$$

Next, the signal is equalized as:

$$\hat{X}_l(k) = Y_l(k) \cdot C_{ZF}(k) \tag{3.14}$$

3.3. Dual-Mode Design of Phase Error Tracking and compensation

CFO and SCO are the other two data distortion sources for OFDM systems, which are caused mainly by a crystal oscillator frequency mismatch between transceiver and DAC/ADC mismatch. Generally, timing synchronization is applied to compensate these two effects. Nevertheless, other impairments will make the synchronization imperfect. The residual CFO and SCO will cause the data phase rotation in frequency domain and result in inter-carrier interference (ICI). In case of a coherent demodulation scheme, the error due to the rotation of a signal constellation will be fatal for transmission bursts, because the accumulated phase rotation will shift the constellation point to cross the decision boundary. It will cause high error rates and therefore the phase error tracking (PET) is applied in OFDM systems for phase rotation tracking and compensation.

Following the eq. 3.3, after doing the equalization, the equalized data can be

simplified as:

$$Y_l(k) = \alpha' \; X_l(k) e^{[j2\pi l \phi_k (T_u+T_g)/T_u]} + W'_{l,k} \tag{3.15}$$

Where α' is attenuation factor, and $W'_{l,k}$ is AWGN noise and another non-ideal effect. The phase rotation of the *l*-th symbol and *k*-th sub-carrier can be derived as:

$$\angle \hat{X}_l(k) = 2\pi l \Delta f (T_u + T_g) + 2\pi \zeta lk \left(\frac{T_u + T_g}{T_g} \right) \tag{3.16}$$

The first term is caused by CFO effect. This phase rotation is constant for all data sub-carriers in an OFDM symbol and increases with symbol index. The second term is caused by SCO effect, which is a linear phase rotation with sub-carrier index. This also increases with symbol index. So, the PET is used to track the mean phase error caused and phase error slope caused by these two effects.

The PET is designed based on the known pilot sub-carriers. In order to achieve correct tracking of phase error exceeding $\pm\pi$, the pre-compensation [10] is added in the PET. Before PET, the pilot sub-carriers will first be compensated with the phase error tracked in the previous OFDM symbols. Therefore, only the difference of the phase error between previous and preset OFDM symbols needs to be tracked with pilot sub-carriers. This will enhance the PET accuracy. The PET algorithm with pre-compensation is given as:

$$\Delta\theta_{l,K} = \begin{cases} \theta_{l,K} & \text{as } l = 1 \\ \theta_{l,K} - \varphi_{l-1} - K \cdot \gamma_{l-1} & \text{otherwise} \end{cases}$$
$$K_{UWB} \in \{5, 15, 25, 35, 45, 55, -5, -15, -25, -35, -45, -55\}$$
$$K_{WIMAX} \in \{13, 38, 63, 88, -13, -38, -63, -88\} \quad (3.17)$$

Where K is the pilot index list, for UWB system, $K=K_{UWB}$, for WIMAX system, $K=K_{WIMAX}$, l=1 means the first received OFDM symbol, $\theta_{l,K}$ is the detected phase error of l-th OFDM symbol, $\Delta\theta_{l,K}$ is defined as the pilot phase after pre-compensation with the previous tracked phase error $\varphi_{l-1} + K \cdot \gamma_{l-1}$.

Next, use the pre-compensation pilot phase to calculate the mean phase error φ_l, which can be shown in eq. 3.18 and phase error slope γ_l, which can be shown in eq. 3.19, and the related parameters for UWB and WIMAX systems are shown in eq. 3.20.

$$\varphi_l = \begin{cases} \frac{1}{p}\sum_K \Delta\theta_{l,K} & \text{as } l = 1 \\ \frac{1}{p}\sum_K \Delta\theta_{l,K} + \varphi_{l-1} & \text{otherwise} \end{cases} \quad (3.18)$$

where p is the number of pilot sub-carriers, φ_{l-1} is previous tracked mean phase error.

$$\gamma_l = \begin{cases} \frac{\sum_{K^+} \Delta\theta_{l,K} - \sum_{K^-} \Delta\theta_{l,K}}{C} & \text{as } l = 1 \\ W_\gamma \frac{\sum_{K^+} \Delta\theta_{l,K} - \sum_{K^-} \Delta\theta_{l,K}}{C} + \gamma_{l-1} & \text{otherwise} \end{cases} \quad (3.19)$$

where γ_{l-1} is the previous, W_γ , C are constant terms, K^+ is index list of positive pilot sub-carriers , K^- is index list of negative pilot sub-carriers.

$$
\begin{aligned}
&K_{UWB}{}^{+} = \{5,15,25,35,45,55\} && K_{WIMAX}{}^{+} = \{13,38,63,88\} \\
&K_{UWB}{}^{-} = \{-5,-15,-25,-35,-45,-55\} && K_{WIMAX}{}^{-} = \{-13,-38,-63,-88\} \\
&C = 360 \quad p = 12 \quad \textit{for UWB} \\
&C = 404 \quad p = 8 \quad \textit{for WIMAX}
\end{aligned}
\tag{3.20}
$$

To consider the hardware complexity, the proposed phase error tracker has the advantage of reducing the multiplicative computation. In the pilot phase pre-compensation part, it only needs one multiplier. Using mean-average method, it only needs to do constant multiplication of two times in each OFDM symbol.

After PET, the data sub-carriers are compensated according to the tracked phase error, which can be indicated as:

$$\tilde{X}_l(k) = \hat{X}_l(k) \cdot \exp(-j(\varphi_l + k\gamma_l)) \tag{3.21}$$

According to Fig. 3.1, after doing compensation, the data $\tilde{X}_l(k)$ is sent to the De-Mapper.

3.4. Modified-NLMS Channel Tracking

In WIMAX system, only even sub-carriers are utilized in long preamble. Consequently, interpolator is used to get the CFR of odd sub-carriers. Because the ideal interpolator is not practical, there is some aliasing effect occurred in interpolation. Aliasing effect will increase the channel estimation error, and degrade

the performance of equalizer. Otherwise, noise, interference and time-variant characteristic will also increase the channel estimation error. Consequently, channel tracker is applied to mitigate the above non-ideal effects and enhance the accuracy of channel estimation.

Standard LMS methodology suffers from a gradient noise amplification problem. To overcome this difficulty, NLMS methodology normalizes the adjustment of tap-weight vector. But, in OFDM system, residual CFO and SCO will result in phase rotation in frequency domain. The traditional NLMS methodology can not be directly used. So, the modified-NLMS methodology is proposed with consideration the phase rotation. Following is the detail algorithm of proposed modified-NLMS channel tracking.

The equalized signal after compensating with tracked phase error is sent into slicer (map the signal to nearest constellation point according to modulation type) to compute the decision signal $\overline{X}_l(k)$. For each sub-carrier k, a single tap frequency domain NLMS filter is used. The modified-NLMS error $E_l(k)$ is as follows:

$$E_l(k) = Y_l(k) \cdot \exp(-j(\varphi_l + k\gamma_l) - \overline{X}_l(k) \cdot H_{l-1}(k) \tag{3.22}$$

Where $Y_l(k)$ is unequalized signal of l-th OFDM symbol, $\varphi_l + k\gamma_l$ is the compensated phase error com from PET, $H_{l-1}(k)$ is the previous estimated CFR.

The gradient at sub-carrier k ($\Delta H_l(k)$) of l-th symbol is given by:

$$\Delta H_l(k) = E_l(k) \cdot \frac{\overline{X}_l^*(k)}{\left|\overline{X}_l(k)^2\right|} \tag{3.23}$$

Finally, using the gradient and previous estimated CFR, the update eq is given as:

$$H_l(k) = H_{l-1}(k) + \mu \cdot \Delta H_l(k) \tag{3.24}$$

Where μ is the constant gain.

Then, the updated CFR $H_l(k)$ can be used for next OFDM symbol.

Chapter 4.
Simulation Result and Performance Analysis

In order to verify the proposed design, complete system platforms are established according to the UWB standard (802.15.3a) and the fixed WIMAX standard (802.16d) on Matlab. The platform has been introduced in chapter 1. Channel estimation accuracy, PET performance, and system performance will be simulated and compare to system constraint of two standards.

4.1. Performance Analysis of the Proposed Dual-Mode Channel Equalizer for UWB system

To analyze the performance of a proposed scheme, we simulate the PER (%) for different SNR and different CFO, SCO value with CFO and SCO variation being considered. The simulation is processed with multi-paths CM2 channel with data rate 480 (Mb/s). The simulation result is shown in Fig. 4.1. The cross-section view for PER (%) with different CFO, SCO values is shown in Fig. 4.2. From the simulation result, it shows that the proposed PET can track the phase error correctly and compensate the phase error under 60 ppm of CFO, SCO value. Above 60 ppm of CFO, SCO value, resulted ICI and phase error will increase grossly to degrade the system performance. Under IEEE 802.15.3a demanded [2], the CFO, SCO value should be less than total 40 ppm (±20 ppm), and the proposed PET can track the phase error accurately.

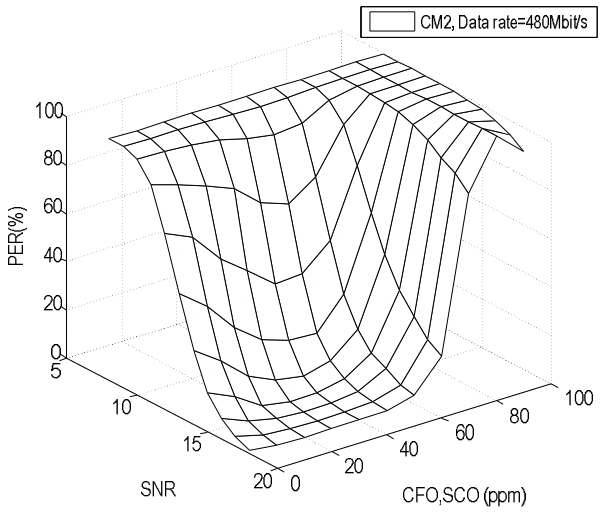

Fig. 4.1 PER (%) simulation for different SNR and CFO, SCO value under CM2, data rate 480Mb/s

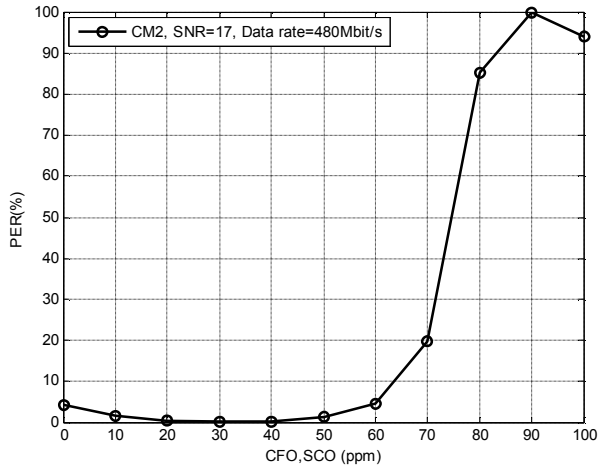

Fig. 4.2 PER (%) simulation result with different CFO, SCO value in CM2

In most WLAN and WPAN systems, a PER less than 8% is required. Therefore, PER 8% can be the indication of system performance. The PER (%) with different transmission mode and different channel model are shown in Fig. 4.3. and Fig. 4.4. Simulation results show that for channel model CM4, data rate 110Mbit/s, with the requirement of 8% PER, the proposed design can achieve this demand at SNR 6.98dB. For transmission in AWGN, the proposed scheme can get this demand at

SNR 2.82dB. The comparison of simulation results with system constraint and references is shown in Table 4.1. It shows that the proposed design can achieve 1.36dB to 7.25dB gain in SNR for different simulation conditions.

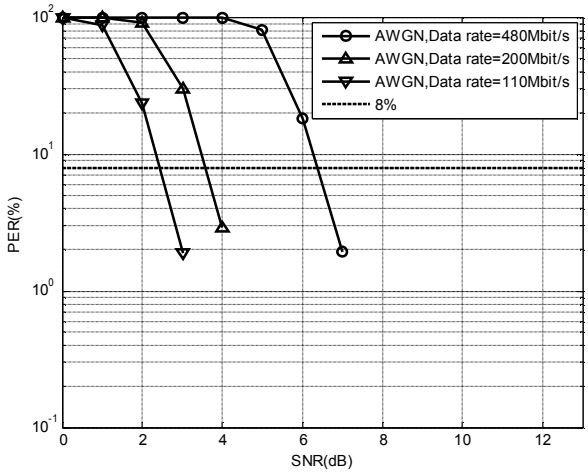

Fig. 4.3 PER (%) simulation result for different data rates in AWGN channel with 40 ppm of CFO, SCO value

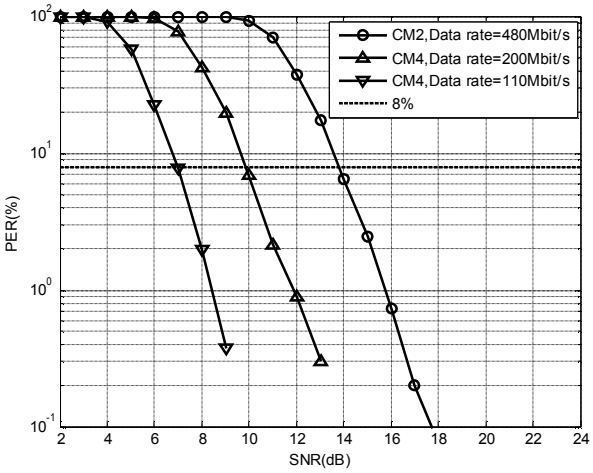

Fig. 4.4 PER (%) simulation result for different data rates and channel model with 40 ppm of CFO, SCO value

Table 4.1 –Performance Result for UWB system

Entry	Proposed	[11]	[12]	System Constraint
AWGN Data rate=200Mbits/s	3.8 dB	3.8 dB	4.11 dB	5.16 dB
AWGN Data rate=480Mbits/s	6.65 dB	7.2 dB	5.03 dB	9.66 dB
CM4 Channel &AWGN Data rate=200Mbits/s	9.91 dB	14.2 dB	14.18 dB	15.1 dB
CM2 Channel &AWGN Data rate=480Mbits/s	13.85 dB	18.5 dB	15.01 dB	21.1 dB

It should be noted that under the worst environment, CM4, the proposed dual-mode channel equalizer will have 5.19dB gain. In the case of receiving data rate of 480Mbit/s, it will have 7.25dB gain. Hence, the proposed joint scheme makes the receiver more robust to CFO and SCO effects and could suppress the error rate at low SNR with high data rate receiving.

4.2. Performance Analysis of the Proposed Dual-Mode Channel Equalizer for WIMAX system

In WIMAX system, the accuracy of channel estimation is a key factor for system performance. To analyze the accuracy of channel estimation, mean-square-error (MSE) between estimated CFR and real CFR is measured. Performance of proposed modified-NLMS channel tracker is simulated with condition under SUI-3 channel, 64-QAM modulation. Following is the comparison of MSE between using modified-NLMS channel tracker and without modified-NLMS channel tracker.

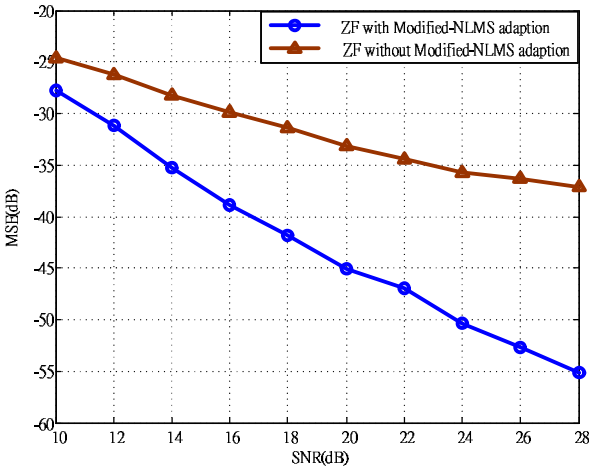

Fig. 4.5 MSE analysis of Modified-NLMS channel tracker

The proposed modified-NLMS channel tracker contributes 3~18dB gain in MSE compared with only ZF channel estimation. Fig. 4.6 shows the channel estimation error from sub-carrier number 70 to sub-carrier number 110, between ideal CFR, using modified-NLMS channel tracker and without modified-NLMS channel tracker.

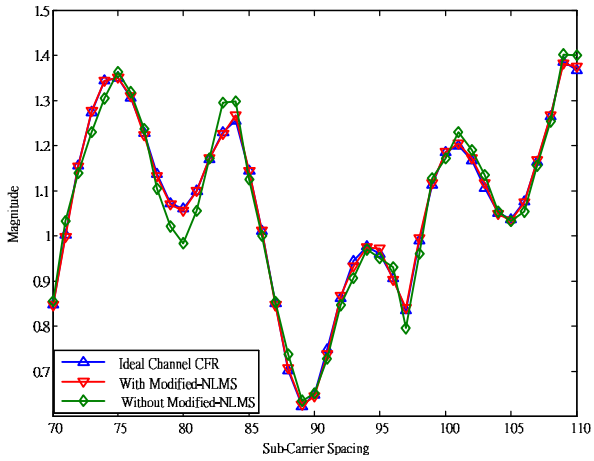

Fig. 4.6 Channel Estimation Error from sub-carrier number 70 to 110

The rate of convergence of modified-NLMS channel tracker depends on the step size. Smaller step size will converge much slower than larger step size. But, smaller step size will contribute smaller MSE than larger step size. Following is the learning curve of proposed modified-NLMS channel tracker with 300 iterations. In this simulation, we select step size with the value equal to 0.0085.

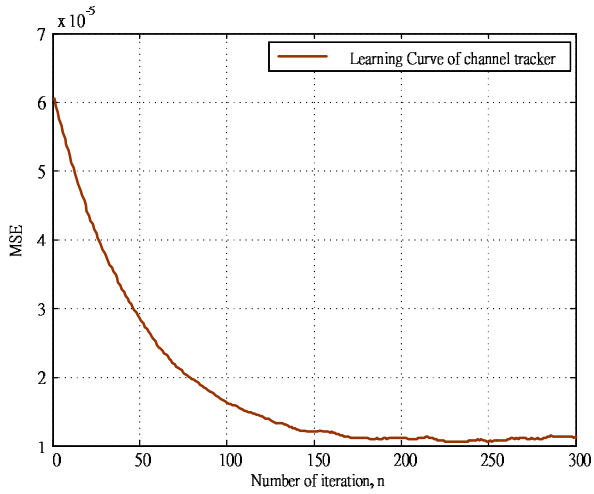

Fig. 4.7 Learning Curve for modified-NLMS channel tracker

Fig. 4.8 shows the bit error rate (BER) with modified-NLMS channel tracker and without modified-NLMS channel tracker under SUI-3 channel, 64-QAM modulation, CFO=0.1 ppm, SCO=16 ppm.

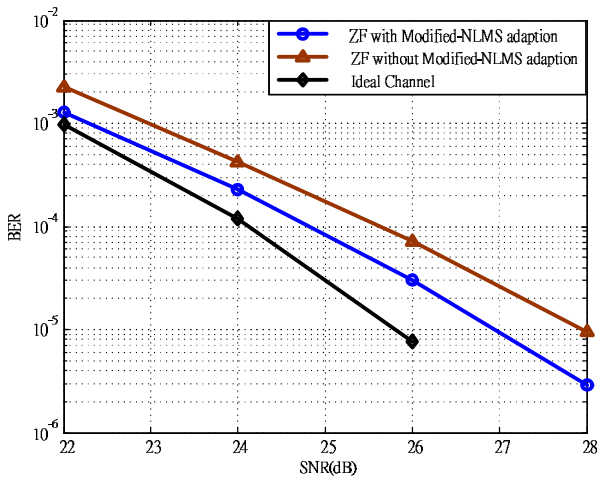

Fig. 4.8 BER Comparison

As it can be seen from Fig. 4.8, design with proposed modified-NLMS channel tracker can contribute 1 dB SNR gain than design without modified-NLMS channel tracker. And, by using modified-NLMS channel tracker, it only result 1 dB SNR loss comparing to use ideal channel. Under different simulation conditions, modified-NLMS channel tracker can contribute different SNR gain. From simulation results, modified-NLMS channel tracker can contribute 1~1.5 dB SNR gain with different simulation conditions.

In 802.16d standard, CFO, SCO value should less than ±8 ppm. With the aid of synchronization, we assume the residual CFO is 0.1 ppm. The BER curves of different transmission mode under SUI-1 to SUI-3 channel, system bandwidth=20MHz, CFO=0.1 ppm, SCO=16 ppm are shown in Fig. 4.9, Fig. 4.10, and Fig. 4.11. Table 4.2 shows the required SNR to attain $10^{\wedge -6}$ BER under SUI-3 channel, and also shows the comparison with reference and system constraint.

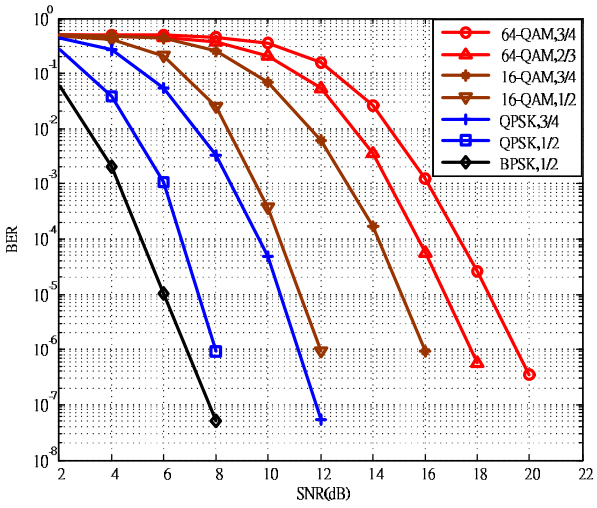

Fig. 4.9 BER performance under Bandwidth=20 MHz,

CFO=0.1 ppm, SCO=16 ppm, SUI-1 channel

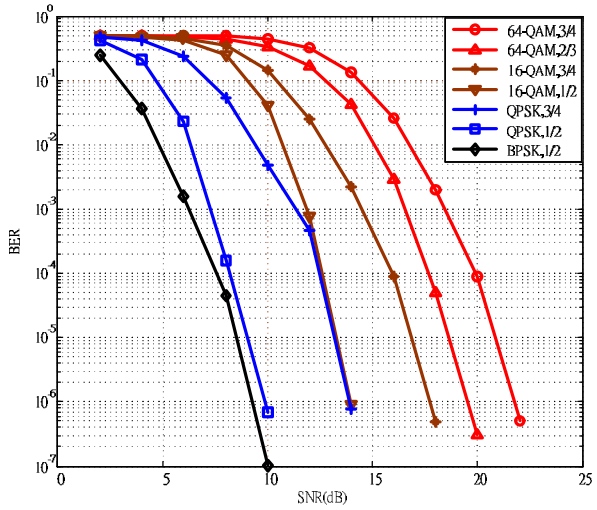

Fig. 4.10 BER performance under Bandwidth=20 MHz,

CFO=0.1 ppm, SCO=16 ppm, SUI-2 channel

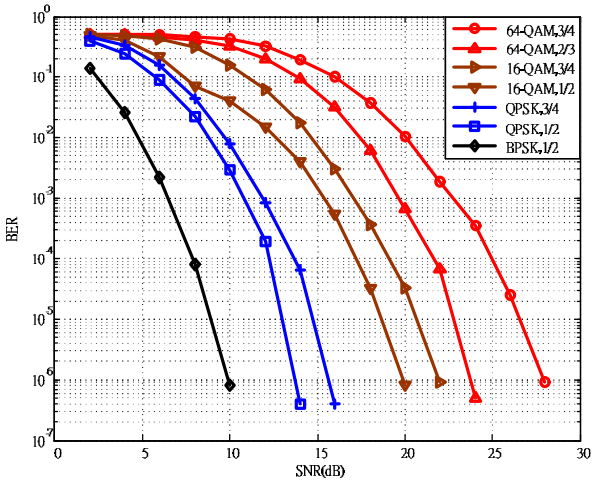

Fig. 4.11 BER performance under Bandwidth=20 MHz,

CFO=0.1 ppm, SCO=16 ppm, SUI-3 channel

Table 4.2 –Performance Result for WIMAX system

Entry	Proposed	[13]	System Constraint
BPSK, Code Rate=1/2	10 dB	None	11.4 dB
QPSK, Code Rate=1/2	13.7 dB	13.8 dB	14.4 dB
QPSK, Code Rate=3/4	15.7 dB	19.6 dB	16.2 dB
16-QAM, Code Rate=1/2	20 dB	18.8 dB	21.4 dB
16-QAM, Code Rate=3/4	22 dB	25.6 dB	23.2 dB
64-QAM, Code Rate=2/3	23.8 dB	29.2 dB	27.7 dB
64-QAM, Code Rate=3/4	27.9 dB	31.5 dB	29.4 dB

From Table 4.2, it can be shown that the proposed dual-mode channel equalizer for WIMAX application can contribute 0.5~3.9dB SNR gain in different simulation conditions.

Chapter 5.
Hardware Implementation

5.1. Signal Flow of Dual-Mode Channel Equalizer

The signal flow of proposed dual-mode channel equalizer for UWB system is shown in Fig. 5.1. In the beginning of receiving, it estimates the CFR H_E (k) by two preambles Y_{L1} (k) and Y_{L2} (k). With the knowledge of these known preambles, the noise power σ_E^2 can be estimated. Then the estimated CFR will be passed through the smoothing filter to reduce the noise effect in channel estimation. After that, the CFR is stored in ram for the following equalization. In the equalization part, it uses the estimated noise power (σ_E^2) and the estimated CFR ($H_S(k)$) to equalize received data $Y_l(k)$ under MMSE methodology. After doing equalization, the data phase will be extracted and sent to PET. In PET part, the phase error will be estimated by pilot sub-carriers. After that, the data sub-carriers are compensated according to these estimated phase errors. Finally, the compensated data sub-carriers are sent to De-Mapper.

For WIMAX system, signal flow is shown in Fig. 5.2. Except for the raised-cosine interpolator, modified-NLMS channel tracker, the signal flow compared to UWB is almost the same. Consequently, most functional blocks, such as divider, smoothing filter, PET, $\tan^{-1}$ ...etc, can be reused to save hardware resource.

2-parallelism architecture is used to meet high sample rate up to 528 MHz for UWB. The architecture of each functional block is introduced as following sections.

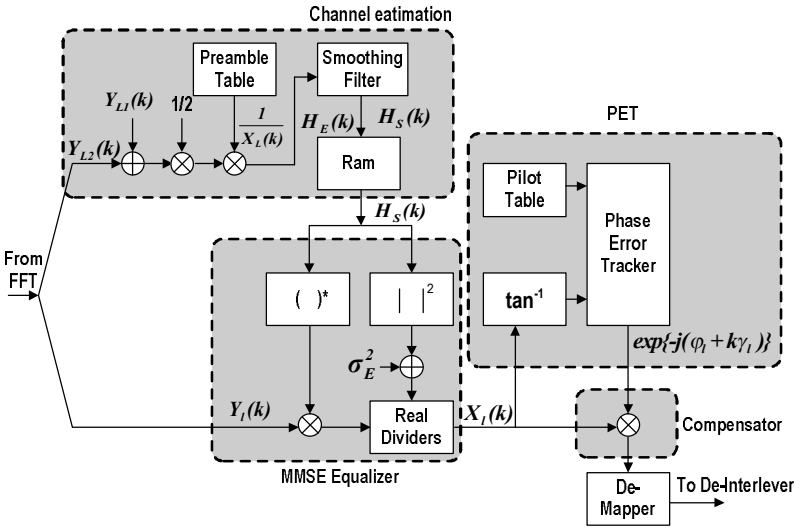

Fig. 5.1 Signal Flow of Proposed Channel Equalizer for UWB

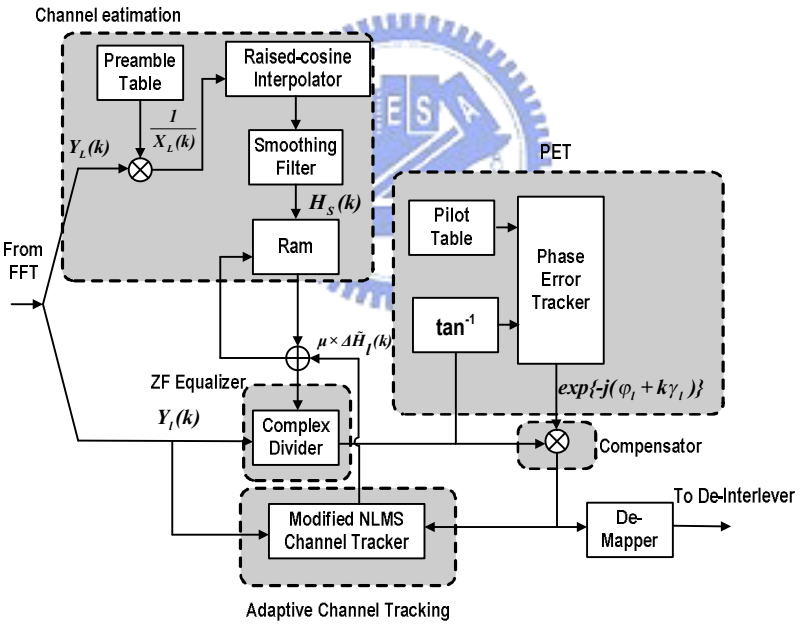

Fig. 5.2 Signal Flow of Proposed Channel Equalizer for WIMAX

5.2. Architecture of Dual-Mode Channel Estimator

Fig 5.3 shows the architecture of dual-mode channel estimator. In UWB mode, dual-mode channel estimator will turn on two parallel data paths. According to pre-defined UWB preamble, look-up table (LUT) combined with following adder and multiplier performs the ZF channel estimation. In this mode, control circuit selects C1 constant ($\sqrt{2}$) as an input to the multiplier. Once ZF channel estimation has been done, the estimated CFR will be stored in UWB ram. In WIMAX mode, maximum sample rate is only 32MHz. In order to save power consumption, only parallel 1st data path is turned on. In this mode, control circuit selects C2 constant ($1/\sqrt{2}$) as an input to the multiplier. After doing ZF channel estimation, the signal will be sent into 6-taps raised-cosine interpolator to interpolate the CFR of odd data sub-carriers. After doing interpolation, CFR of all data sub-carriers are stored in WIMAX ram.

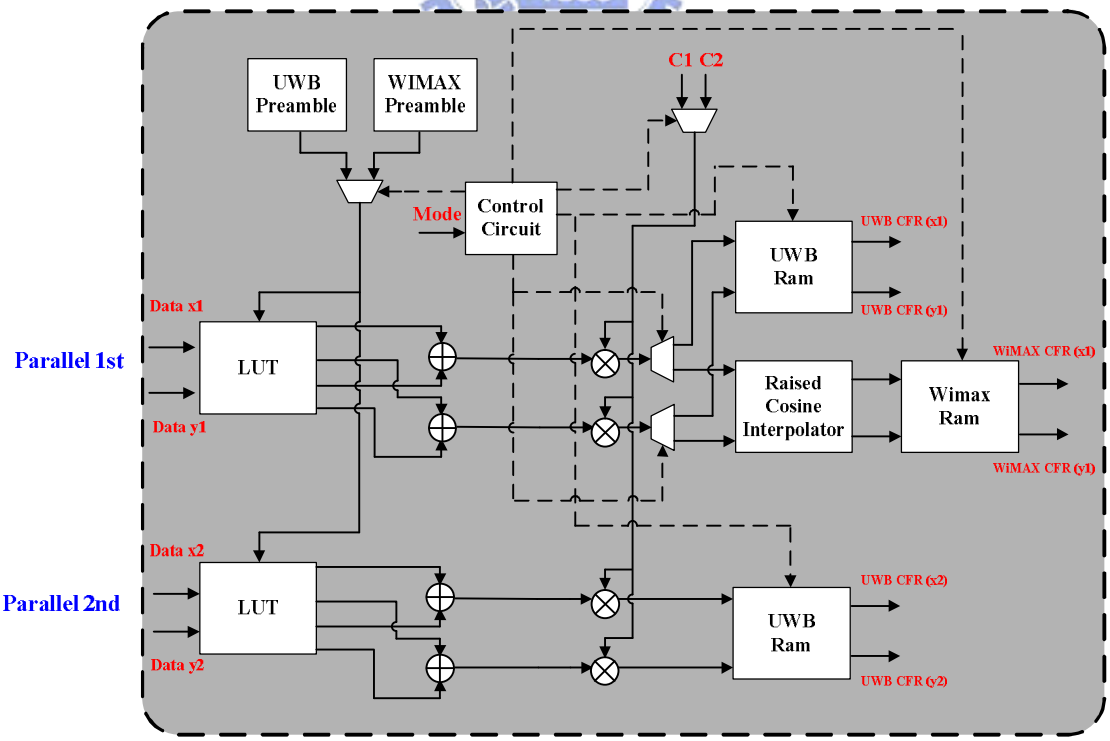

Fig. 5.3 Architecture of proposed dual-mode channel estimator

For UWB mode, MMSE equalizer is used to equalize the distorted signal. To use MMSE methodology, information of noise power is needed. So, two received preambles of UWB are used to estimate the noise power in proposed dual-mode channel estimator. Fig. 5.4 shows the architecture of noise power estimator. When first received preamble is coming, it will be stored in UWB ram. When second received preamble is coming, first preamble will be read out. And, these two preambles are sent to subtractor. These subtracted values are then sent to the square circuit, calculating the noise power of each sub-carrier. Finally, the mean average of noise power which can be used for following MMSE equalization is calculated.

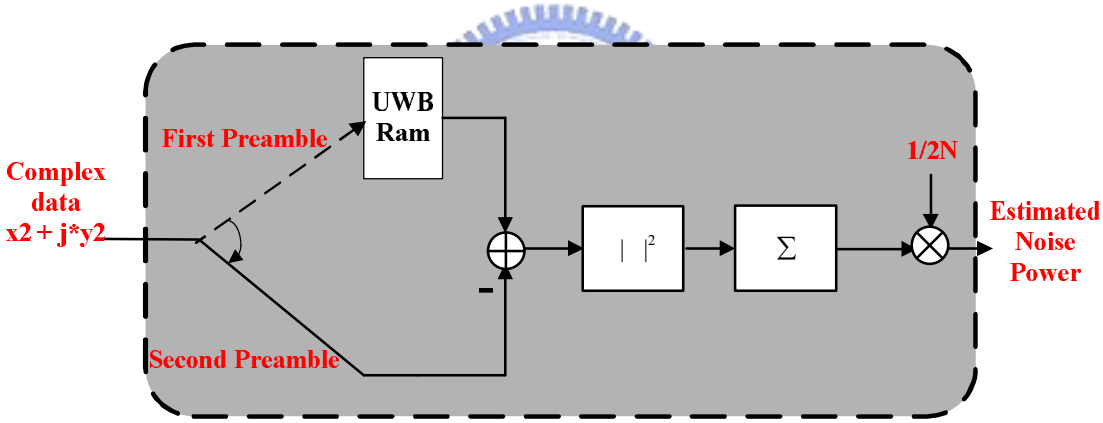

Fig. 5.4 Architecture of noise power estimator

For WIMAX system, only even sub-carriers are utilized in long preamble. Interpolator is needed to get the CFR of odd sub-carriers. Fig. 5.5 shows the architecture of 6-tap raised-cosine interpolator. Where C1, C2, C3 are constant terms calculated by raised-cosine function. Fig. 5.6 shows the operation of the 6-tap raised-cosine interpolator. At the beginning, the CFR of DC sub-carrier is interpolated at first. Then, CFR of DC sub-carrier can be used to interpolate other CFR of odd sub-carriers.

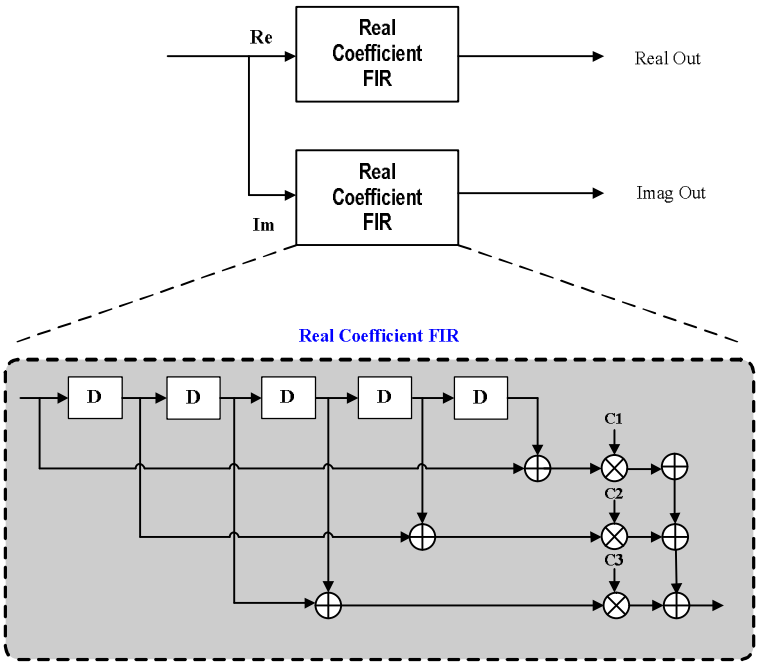

Fig. 5.5 Architecture of 6-tap raised-cosine interpolator

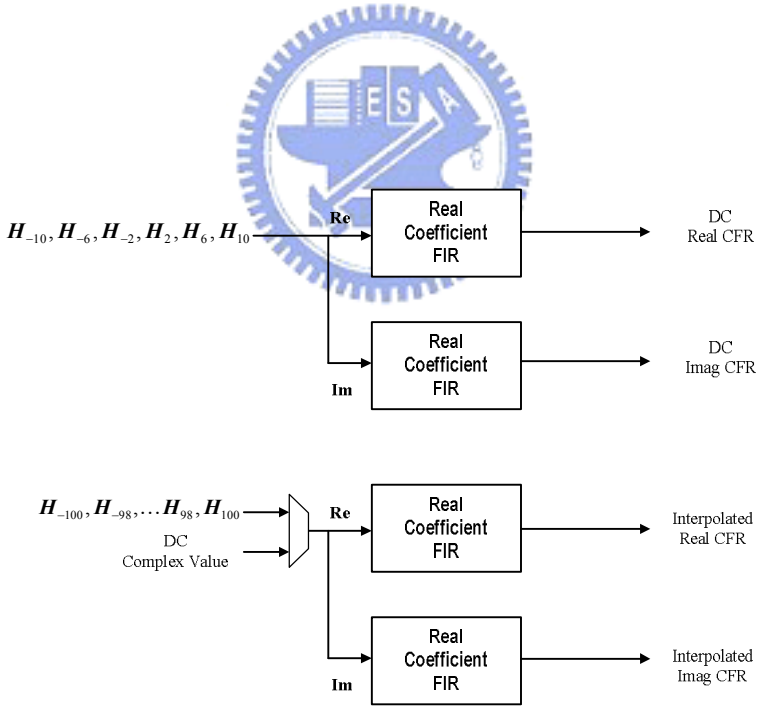

Fig. 5.6 Operation of 6-tap raised-cosine interpolator

5.3. Architecture of Dual-Mode Equalizer

For frequency domain one-tap equalizer, operation of MMSE equalization and ZF equalization is just complex division. Difference of MMSE equalization and ZF equalization is the usage of estimated noise power. For MMSE equalization, estimated noise power is added in denominator and then sent to the real divider. For ZF equalization, denominator is added with zero value.

For UWB mode, MMSE equalizer is used to equalize distorted signals. Under consideration of high sampling rate for UWB application, two parallel data paths are turned on to do MMSE equalization. For WIMAX mode, to save power consumption, only parallel 1st data path is turned on. The architecture of proposed dual-mode equalizer is shown in Fig. 5.7. The design of real divider is introduced below.

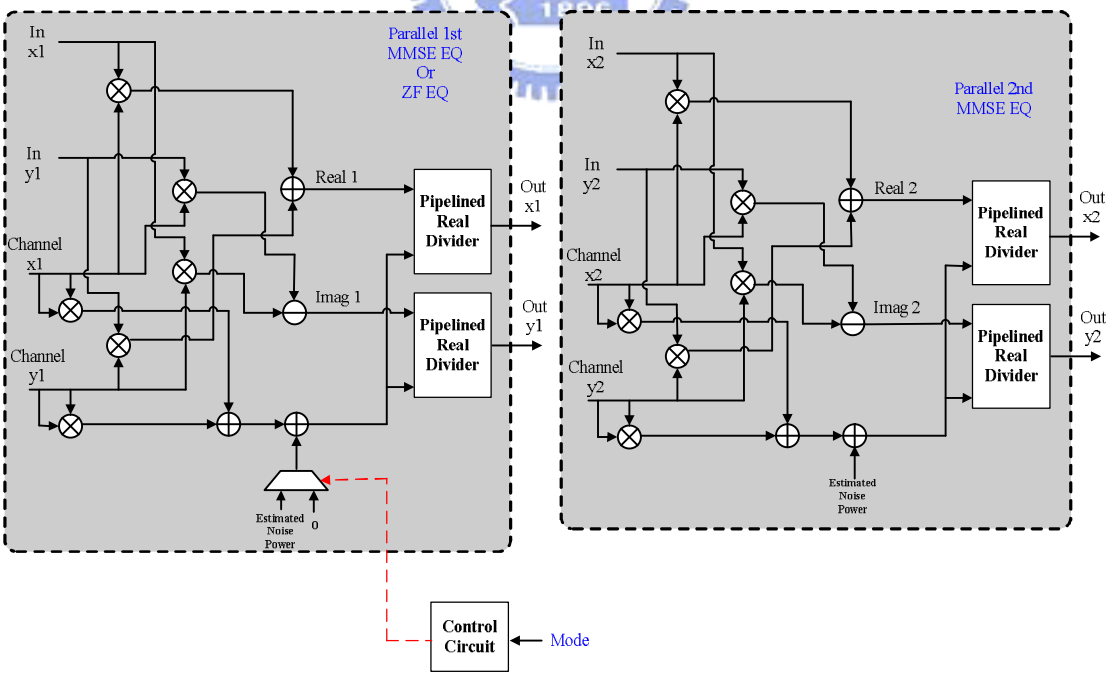

Fig. 5.7 Architecture of dual-mode equalizer

For real divider design [14], the multi-cycle division is used. The concept is to separate one cycle into many cycles and get quotient by iterative subtraction. At first, we define the format of the signed number, where m is the total bits and n is the bits of decimal. Assuming the format of input signal is (m_1,n_1), and the format of output signal is (m_2,n_2). At first, in order to normalize the quotient to saturation point, dividend is shifting (m_2-n_2-1) bits right. And, in first stage of single iterative unit, A is the dividend >> (m_2-n_2-1), and B is the divisor. If A is larger than B, the q(k) will be "1" else not, it can be determined by the sign bit of subtraction result. q(k) is just the inverse of the sign bit of sub. Then, we update A by (sub<<1) or (A<<1) depends on the sign bit of sub. Updated A, B and q(k) are then buffered in pipelined register, and will be sent to the next iterative unit to get the next bit of quotient. The relationship is shown in Table 5.1. The architecture of pipelined real divider is shown in Fig. 5.8.

Table 5.1 – Relationship of operation in single iterative unit

	Sub>=0	Sub<0
Sign bit	0	1
q(k)	1	0
Updated "A"	Sub<<1	A<<1

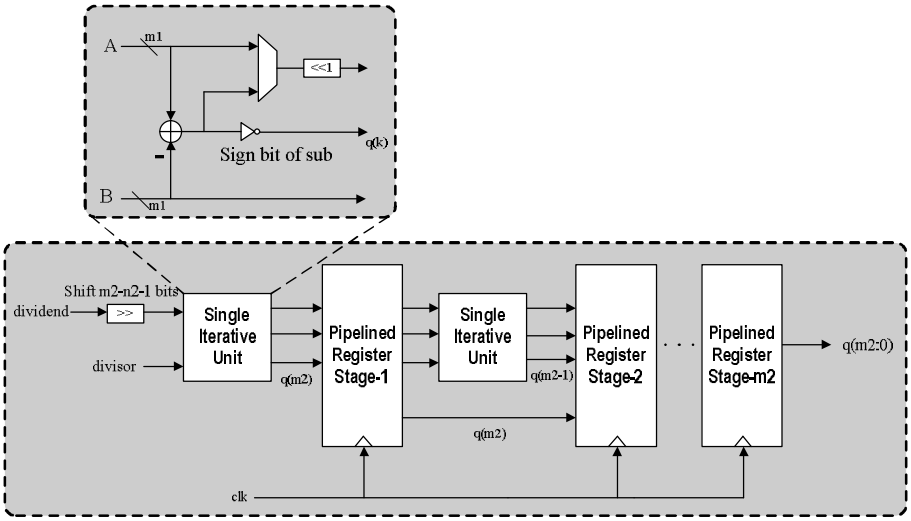

Fig. 5.8 Architecture of pipelined real divider

5.4. Architecture of Dual-Mode Phase Error Tracker and Compensator

Fig. 5.9 shows the architecture of proposed dual-mode phase error tracker and compensator. In this design, Cordic (Coordinate Rotation Digital Computer) is used to extract the phase information of the signal. And, De-Cordic has two different utilities. One is used to covert the signal in Magnitude-Phase domain to Real-Imaginary domain, and the other is used to rotate the signal according to the given phase. The algorithm of Cordic, De-Cordic will be introduced later. As it can be seen from the Fig. 5.9, the phase of pilot sub-carrier extracted by Cordic is pre-compensating with the previous tracker phase error ($\varphi_{l-1} + K \cdot \gamma_{l-1}$). And, this pre-compensated value is use to calculate the mean phase error and phase error slope. Then, mean phase error and phase error slope are combined by phase error combiner to form the total tracked phase error. Then, tracked phase error can be used to compensate the received data by data compensator. Finally, compensated data is passing through De-Cordic to return Magnitude-Phase domain to Real-Imaginary domain. Also, in UWB mode, two data paths are turned on. In WIMAX mode, only upper data path, shown in Fig. 5.9, is turned on to save the power consumption.

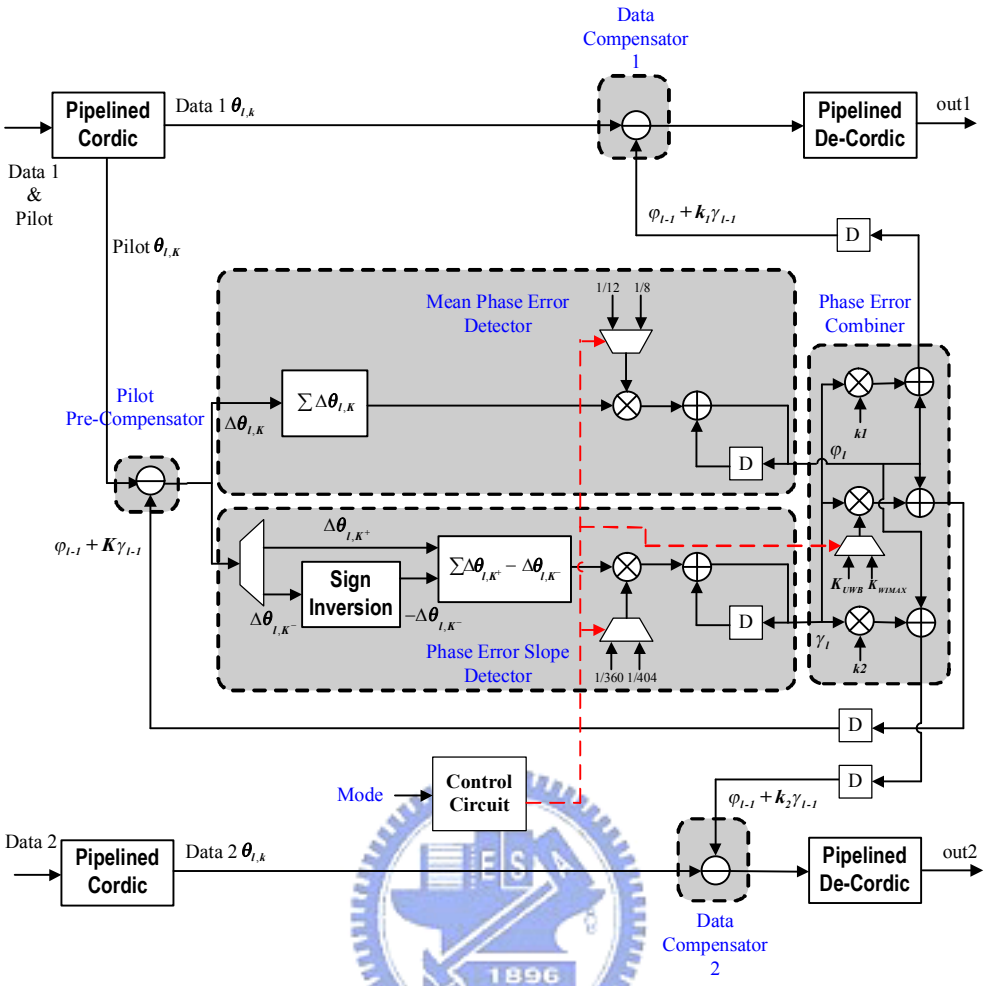

Fig. 5.9 Architecture of dual-mode phase error tracker and compensator

Cordic [15] is an iterative algorithm used to acquire amplitude and angle from a 2x1 signal vector (Rectangular-to-polar mode). General methods to realize these functions need LUTs, complex-valued multipliers, and dividers. Cordic reduces complexity by using simple components, like adders, comparators and shifters. The accuracy of the Cordic increases with larger iterative number. After the last iteration has been done, the signal is multiplied by the factor A. Following is the *i*-th iterative formula of Cordic algorithm:

$$
\begin{aligned}
& d_i = sign[y(i)] \\
& \begin{bmatrix} x(i+1) \\ y(i+1) \end{bmatrix} = \begin{bmatrix} 1 & d_i \cdot 2^{-i} \\ -d_i \cdot 2^{-i} & 1 \end{bmatrix} \begin{bmatrix} x(i) \\ y(i) \end{bmatrix} \\
& \theta_i = \tan^{-1}(2^{-i}) \\
& \theta = \sum_i d_i \theta_i \\
& A = \frac{A_i}{\prod_i k_m(i)} \qquad k_m(i) = \sqrt{1 + 2^{-2i}}
\end{aligned}
\tag{5.1}
$$

Cordic is deigned by 10-stage pipeline to increase the throughput. Fig. 5.10 shows the architecture of pipelined Cordic.

De-Cordic is designed to rotate a 2x1 vector with a certain angle (phase-rotation mode). The algorithm for De-Cordic is the same with the Cordic. So, the architecture of De-Cordic is also the same with Cordic.

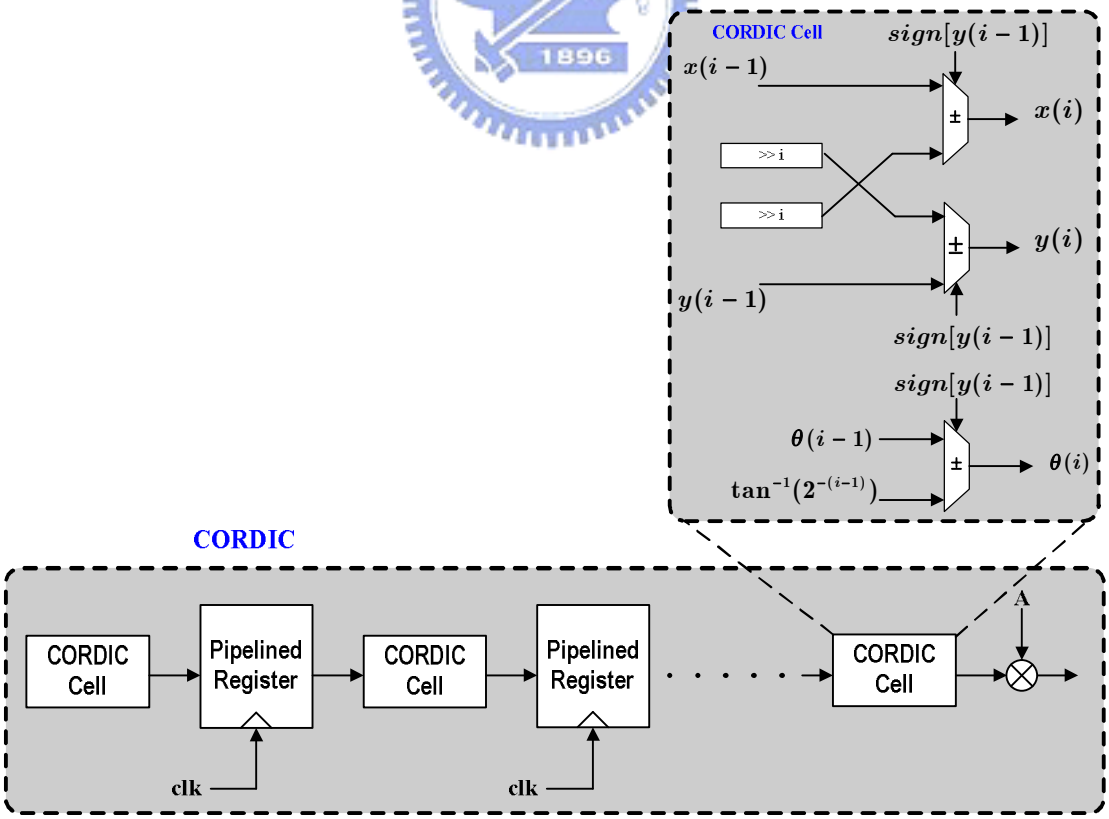

Fig. 5.10 Architecture of pipeline cordic

5.5. Architecture of Modified-NLMS Channel Tracker

In WIMAX system, only even sub-carriers are utilized in long preamble. If the interpolator is not ideal, the aliasing effect will result in channel estimation error. Otherwise, time variant characteristic will also result in channel estimation error. And, channel estimation error will degrade the performance of equalization. So, in WIMAX mode, modified-NLMS channel tracker is turned on to mitigate the channel estimation error. The architecture of modified-NLMS channel tracker is shown in Fig. 5.11. Gradient term calculation part is just a complex divider, which is also used in dual-mode equalizer. And, there are two complex dividers in design of dual-mode equalizer. In WIMAX mode, only one complex divider is turned on and the other is turned off. So we can reuse this idle complex divider to do gradient term calculation and save hardware resource. Based on the same consideration, De-Cordic which is used in phase error tracker and compensator can also be reused. Delay Lines are used to hold on signals. In WIMAX mode, UWB ram is in idle state. So, UWB ram is used to hold on signals which are inputs to modified-NLMS channel tracker.

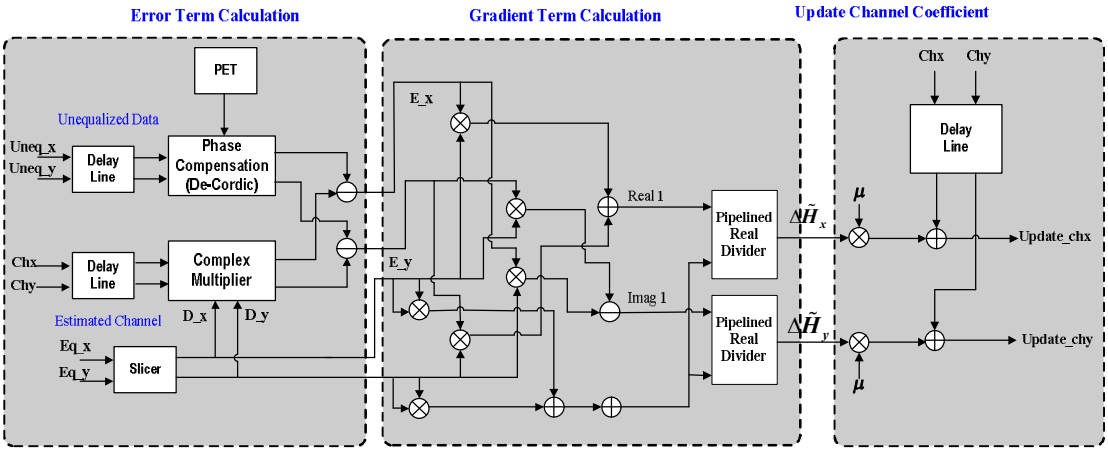

Fig. 5.11 Architecture of modified-NLMS channel tracker

5.6. Architecture of Dual-Mode Channel Equalizer

Following shows the total architecture of proposed dual-mode channel equalizer. In UWB mode, two data paths will be turned on. All signals will pass through the upper paths of multiplexers. In WIMAX mode, all signals will pass through the lower paths of multiplexers.

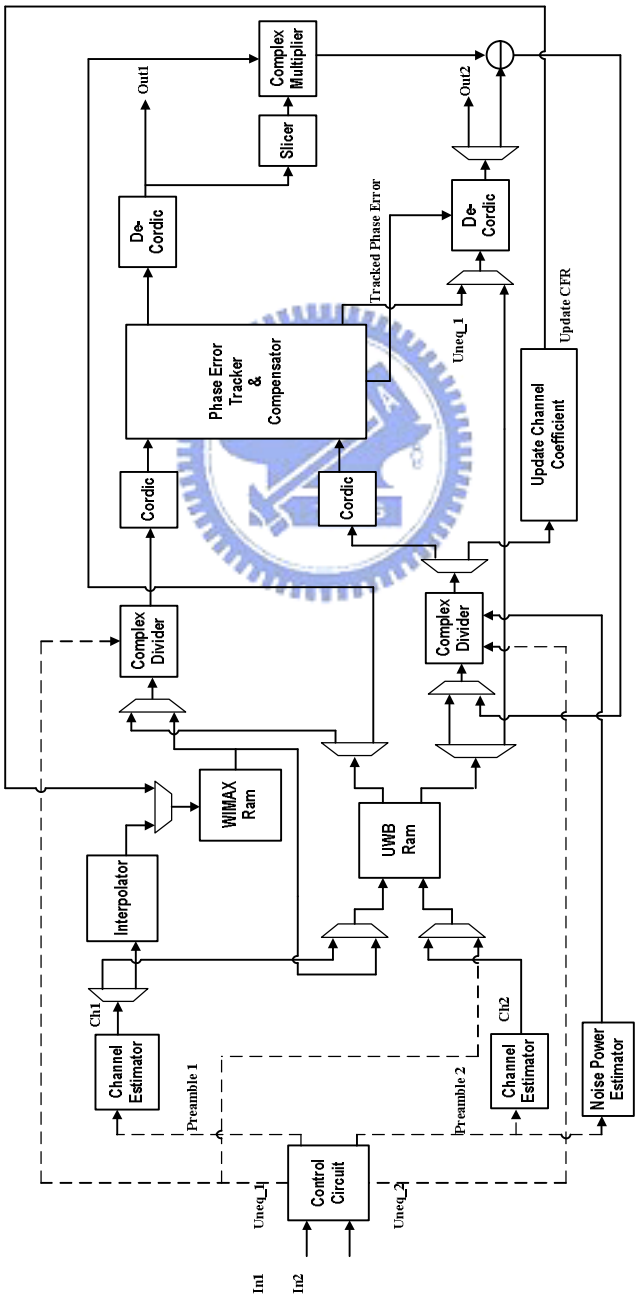

Fig. 5.12 Architecture of Dual-Mode Channel Equalizer

5.7. Implementation Issues

Hardware cost and system performance are trade-off in hardware implementation, so fixed-point simulation will be needed, before the implementation. Following figure shows the simulation result. According to the Fig 5.13, when the resolution is lower than 12 bits, the system performance will degrade seriously. So, 12-bit resolution is chosen to do the hardware implementation.

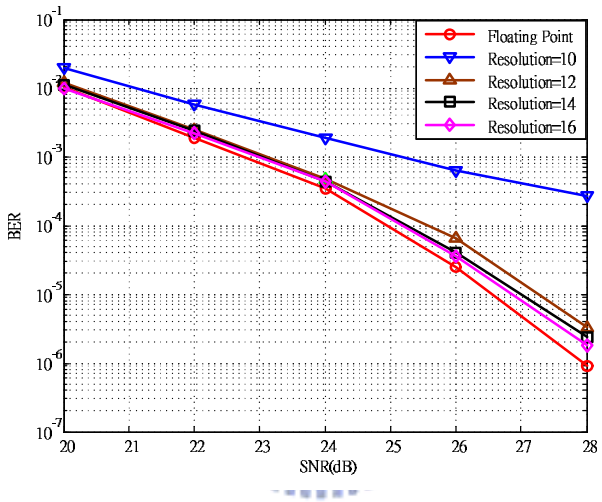

Fig. 5.13 Fixed Point Simulation

5.8. Hardware Implementation Results

In this section, we discuss the implementation of the proposed dual-mode channel equalizer. We use SYNOPSYS design compiler to synthesis the RTL file with UMC 0.18 slow library. All functional blocks are synthesized with clock rate equal to 270 MHz. Gate count of each functional block is shown in Table 5.2. Without considering the dual-mode design, gate count of single-mode channel equalizer for WIMAX and UWB is shown in Table 5.3. As it can be seen from Table

5.2 and Table 5.3, dual-mode channel equalizer utilizes most of common functional blocks can elevate the hardware efficiency and save hardware resource. Gate count of dual-mode channel equalizer which can deal with two different signals for UWB and WIMAX systems is only 130k.

Table 5.2 – Synthesis Report for Each Module

Module	Gate Count
Dual-Mode Channel Estimator + Dual-Mode Equalizer	77103
PET(Cordic*2 +phase error tracking De-Cordic*2)	8478*2 + 9755 8574*2 =43859
Modified-NLMS Channel Tracker	9623
Total Design	130585

Table 5.3 – Synthesis Report for Single-Mode Channel Equalizer

Module	Gate Count
Single-Mode Channel Equalizer for UWB	115552
Single-Mode Channel Equalizer for WIMAX	122706

For WIMAX application, system clock rate is 50MHz and the power consumption of dual-mode channel equalizer is 47.38mW. For UWB application, clock rate is 270 MHz, and corresponding power consumption is 72.56 mW.

5.9. FPGA Prototyping

In FPGA prototyping, the input bit pattern is generated from MATLAB. Then, input the generated bit pattern through emulation tool of VeriComm Pro of SMIMS TECHNOLOGY CORPORATION to FPGA. Then, the resulted waveform will be sent back to the tool of VeriComm Pro to dump the file for checking. For FPGA verification, register file will be used to take place RAM. In UWB system, three bands CFR need be stored and bit resolution of the proposed dual-mode channel equalizer is twelve. So, total bits need to be stored in register file are 3*2*12*128=9216 bits. In proposed dual-mode channel equalizer, we use twelve 12*64 bits of register file to store three bands CFR. For WIMAX application, total bits need to be stored in register file are 2*12*256=6144 bits. So, we use two 12*256 bits of register file to store the WIMAX CFR. The FPGA verification plan is shown in Fig. 5.14. Fig. 5.15 shows the verifying situation. Fig. 5.16 shows the synthesis report for 12*64 bits of register file. Fig. 5.17 shows the synthesis report for 12*256 bits of register file. Fig. 5.18 shows the FPGA synthesis report for proposed dual-mode channel equalizer.

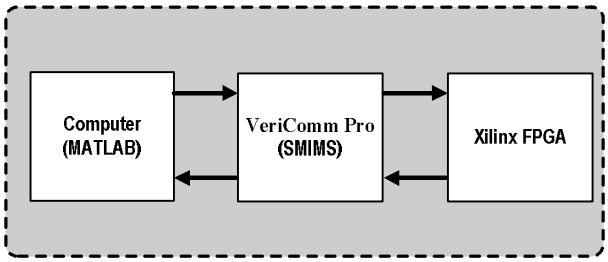

Fig. 5.14 FPGA verification plan

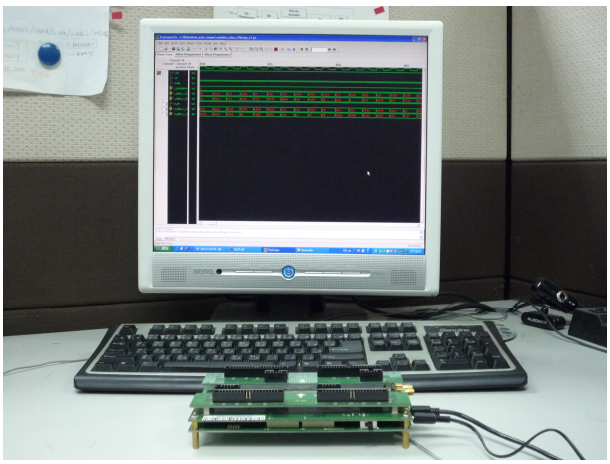

Fig. 5.15 FPGA Board

REGFILE_12_64 Project Status			
Project File:	Regfile_12_64.ise	**Current State:**	Programming File Generated
Module Name:	reg_12_64	• **Errors:**	No Errors
Target Device:	xc4vlx60-10ff1148	• **Warnings:**	40 Warnings
Product Version:	ISE, 8.1i	• **Updated:**	星期一 六月 23 15:07:27 2008

Device Utilization Summary				
Logic Utilization	**Used**	**Available**	**Utilization**	**Note(s)**
Number of Slice Flip Flops	756	53,248	1%	
Number of 4 input LUTs	471	53,248	1%	
Logic Distribution				
Number of occupied Slices	616	26,624	2%	
Number of Slices containing only related logic	616	616	100%	
Number of Slices containing unrelated logic	0	616	0%	
Total Number of 4 input LUTs	471	53,248	1%	
Number of bonded IOBs	66	640	10%	
Number of BUFG/BUFGCTRLs	1	32	3%	
Number used as BUFGs	1			
Number used as BUFGCTRLs	0			
Total equivalent gate count for design	10,146			
Additional JTAG gate count for IOBs	3,168			

Fig. 5.16 Synthesis Report for 12x64 bits of Register file

REGFILE_12_256 Project Status			
Project File:	Regfile_12_256.ise	**Current State:**	Programming File Generated
Module Name:	reg_12_256	• **Errors:**	No Errors
Target Device:	xc4vlx60-10ff1148	• **Warnings:**	40 Warnings
Product Version:	ISE, 8.1i	• **Updated:**	星期一 六月 23 15:08:56 2008

Device Utilization Summary				
Logic Utilization	**Used**	**Available**	**Utilization**	**Note(s)**
Number of Slice Flip Flops	3,060	53,248	5%	
Number of 4 input LUTs	1,871	53,248	3%	
Logic Distribution				
Number of occupied Slices	2,477	26,624	9%	
Number of Slices containing only related logic	2,477	2,477	100%	
Number of Slices containing unrelated logic	0	2,477	0%	
Total Number of 4 input LUTs	1,871	53,248	3%	
Number of bonded IOBs	70	640	10%	
Number of BUFG/BUFGCTRLs	1	32	3%	
Number used as BUFGs	1			
Number used as BUFGCTRLs	0			
Total equivalent gate count for design	40,326			
Additional JTAG gate count for IOBs	3,360			

Fig. 5.17 Synthesis Report for 12x256 bits of Register file

DUAL_MODE_CHANNEL_EQUALIZER_NLMS_V5 Project Status			
Project File:	dual_mode_channel_equalizer_nlms_v5.ise	**Current State:**	Programming File Generated
Module Name:	dual_mode_channel_equalizer	• **Errors:**	No Errors
Target Device:	xc4vlx60-10ff1148	• **Warnings:**	647 Warnings
Product Version:	ISE, 8.1i	• **Updated:**	星期一 六月 23 15:05:17 2008

Device Utilization Summary				
Logic Utilization	**Used**	**Available**	**Utilization**	**Note(s)**
Number of Slice Flip Flops	22,821	53,248	42%	
Number of 4 input LUTs	23,118	53,248	43%	
Logic Distribution				
Number of occupied Slices	20,558	26,624	77%	
Number of Slices containing only related logic	20,558	20,558	100%	
Number of Slices containing unrelated logic	0	20,558	0%	
Total Number 4 input LUTs	23,239	53,248	43%	
Number used as logic	23,118			
Number used as a route-thru	121			
Number of bonded IOBs	103	640	16%	
Number of BUFG/BUFGCTRLs	1	32	3%	
Number used as BUFGs	1			
Number used as BUFGCTRLs	0			
Number of FIFO16/RAMB16s	6	160	3%	
Number used as FIFO16s	0			
Number used as RAMB16s	6			
Total equivalent gate count for design	380,299			
Additional JTAG gate count for IOBs	4,944			

Fig. 5.18 Synthesis Report of Dual-Mode Channel Equalizer

5.10. FPGA Emulation

Fig. 5.19 shows the FPGA emulation result and Fig. 5.20 shows the RTL simulation result. According to these two figures, FPGA emulation result is the same with RTL simulation result.

Fig. 5.19 FPGA Emulation

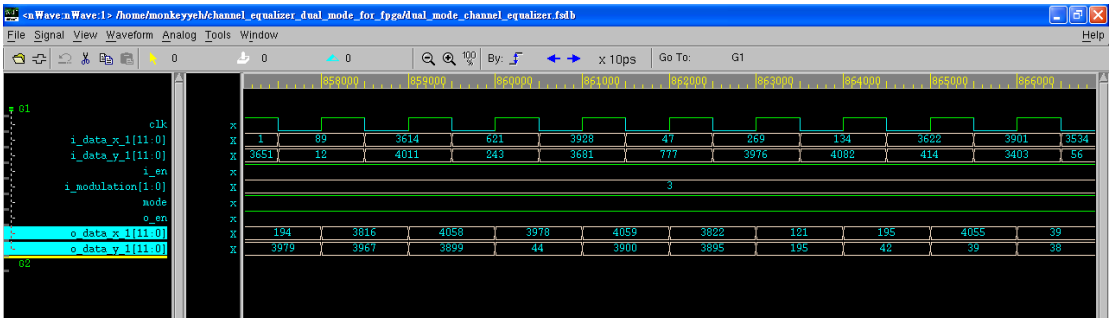

Fig. 5.20 RTl Simulation

FPGA emulation result is sent back to Matlab and plot the constellation diagram. Fig. 5.21 shows the FPGA emulation result under 64-QAM, SUI-2 channel, CFO=0.1 ppm, SCO=16 ppm , SNR=30 dB. Fig. 5.22 shows the floating point simulation result with Matlab under the same conditions. As we can see from these two figures, hardware design of proposed dual-mode channel equalizer can equalize the distorted signal correctly.

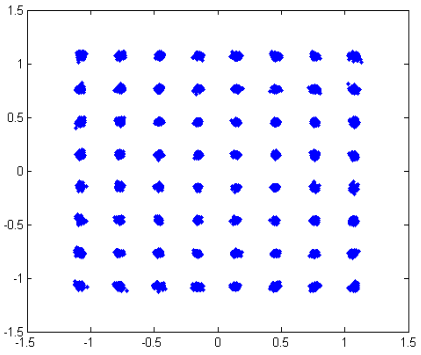

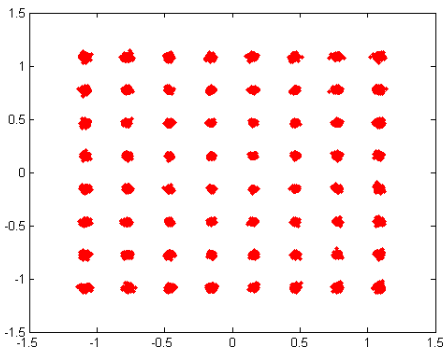

Fig. 5.21 FPGA Emulation Result

Fig. 5.22 Matlab Simulation Result

Chapter 6.
Conclusions and Future Work

6.1. Conclusions

In this thesis, we proposed a dual-mode channel equalizer which can be applied to UWB and WIMAX systems. It is robust to solve multi-path channels, CFO, SCO effect, as well as AWGN. Simulation results show that the proposed dual-mode channel equalizer works even better in harsh channel conditions. In UWB system simulation, the proposed dual-mode channel equalizer can contribute 1.36 ~ 7.25dB gain in SNR for different simulation conditions. Also, for WIMAX system simulation, the proposed dual-mode channel equalizer can also contribute 0.5 ~3.9 dB SNR gain. Moreover, the proposed low complexity PET which uses only pilot sub-carriers to track the phase error is very compatible for all OFDM based system. For hardware implementation, most functional blocks are reused to save hardware resource. 2-parallelism architecture is used to meet high sampling rate up to 528 MHz. And, total equivalent gate count is 130k under SYNOPSYS design compiler with UMC 0.18 slow library.

6.2. Future Work

Develop novel algorithm of dual-mode receiver for UWB and WIMAX systems. Complete other designs of dual-mode receiver, including synchronizer, FFT, LDPC codec, RS codec, Viterbi codec. Resolve more non-ideal effects.

Bibliography

[1] Richard van Nee, Ramjee Prasad, "OFDM for wireless Multimedia Communications," *Artech House*

[2] A. Batra *et al.*, "Multi-band OFDM physical layer proposal for IEEE802.15 Task Group 3a," *IEEE P802.15-04/0943r0-TG3a*, September 2004.

[3] IEEE Std 802.16-2004, Standard For Local and Metropolitan Area Networkd Part 16: Air Interface for Fixed Broadband Wireless Access Systems.

[4] J. Foerster and Q. Li, "UWB channel modeling contribution from Intel," *IEEE P802.15-02/279-SG3a,* June 2002.

[5] "*Channel Model for Fixed Wireless Applications*," IEEE 802.16 Broband Wireless Access Working Group, *802.16.3c-01/29r4*, Jul. 16, 2001

[6] Heinrich Meyr, Marc Moeneclaey, Stefan A. Fechtel "*Digital Comminication Receivers: Synchronization, Channel Estimation, and Signal Processing*" 1998 John Wiley & Sons, Inc.

[7] M. Speth, S. A. Fechtel, G. Fork, and H. Meyr, "Optimum receiver resign for wireless broad-band systems using OFDM-part I," *IEEE Trans. on Comm*, vol. 47, no. 11, pp. 1668-1677, Nov. 1999.

[8] H. Y. Liu, Y. H. Yu, C. J. Hung, T. Y. Hsu, and C. Y. Lee, "Combining adaptive smoothing and decision-directed channel estimation schemes for OFDM WLAN systems," *ISCAS*, vol. 2, pp. 149-152, May. 2003.

[9] Y.C. Lei, "Construction of a Baseband Receiver for IEEE 802.16 OFDM Mode Subscriber Station", Master Thesis, Dept. of Electrical Engineering, National Taiwan University, Taipei, Taiwan, July.2005.

[10] Y. H. Yu, H. Y. Liu, T. Y. Hsu, and C. Y. Lee, "A joint scheme of decision-directed channel estimation and weighted-average phase error tracking for OFDM WLAN systems," *IEEE Asia-Pacific Conference on Circuits and Systems*, vol. 2, pp. 6-9, Dec. 2004.

[11] H. Y. Liu, " *Study on Low-Complexity OFDM-Based Wireless Baseband Transceiver*", PHD Thesis, Dept. of Electrical Engineering, National Chiao Tung University, Taiwan, July.2006

[12] W. R. Chang, " *CORDIC based Equalizer for Ultra-Wide band system*", Master Thesis, Dept. of Electrical Engineering, National Chiao Tung University, Taiwan, July.2006.

[13] S. J. Yang, " Design of a Baseband Transceiver for IEEE 802.16a Subscriver Stations", Master Thesis, Dept. of Electrical Engineering, National Taiwan University, Taipei, Taiwan, 2004.

[14] Y. H. Ma, "*Channel Equalizer for DVB-T/H System*", Master Thesis Dept. of Electrical Engineering, National Chiao Tung University, Taiwan, July.2006.

[15] C. S. Peng, Y. S. Chuang, and K. A. Wen, "CORDIC-based architecture with channel state information for OFDM baseband receiver," *IEEE Transactions on Consumer Electronics*, vol. 51, no. 2, pp. 403-412, May. 2005.

Vita

姓名：葉柏麟

籍貫：桃園縣

生日: 73/09/24

學歷：

國立交通大學電子工程研究所碩士班(系統組)	95/09~97/06
國立交通大學電子物理學系	91/09~95/06
國立武陵高中	88/09~91/06

得獎紀錄:

95 學年度 第二學期電子研究所書卷獎

92 學年度 第二學期電子物理學系書卷獎

發表論文:

Po-Lin Yeh, Kuei-Ann Wen, "**Low Complexity and High Performance Equalizer Design for UWB**," *WCNC2008*